



TECHNISCHE  
UNIVERSITÄT  
DARMSTADT

Bachelorarbeit von Stefan Baltruschat

Soil organic matter and stable carbon isotopes in  
surficial permafrost on Herschel Island, Yukon  
Territories, Canada, Matr.-Nr.: 1712083

Institut für Angewandte Geowissenschaften  
Darmstadt, Januar 2013

---

## Table of Contents

List of Figures .....	III
List of Tables .....	V
Abstract .....	VI
1. Introduction .....	1
1.1 Scientific rationale .....	1
1.2 Aims and objectives .....	3
2. Study Area .....	4
2.1 Geographical setting and geological background .....	4
2.2 Climate and Vegetation .....	6
2.3 Periglacial processes, geomorphology and soil development .....	8
2.4 Ecological unit distribution .....	13
2.5 Site description .....	14
3. Methods .....	16
3.1 Field work .....	17
3.2 Laboratory work .....	17
3.2.1 Moisture Content .....	18
3.2.2 Biogeochemistry: TC, TOC, TN .....	18
3.2.3 Stable carbon isotopes ( $\delta^{13}\text{C}$ ) .....	19
3.3 Statistical analysis .....	20
3.3.1 Regression analysis .....	20
3.3.2 Significant difference .....	21
3.3.3 Principal component analysis (PCA) .....	21
4. Results .....	23
4.1 Presentation of moisture content, biogeochemistry and stable carbon isotopes according to ecological units .....	23
4.1.1 Guillemot unit (PG2150 & PG2151) .....	23
4.1.2 Herschel unit (PG2152, PG2154 & PG2163) .....	25
4.1.3 Komakuk unit (PG2155) .....	27
4.1.4 Orca unit (PG2156 & PG2159) .....	28

---

4.1.5 Plover + Jaeger unit (PG2157 & PG2162) .....	30
4.1.6 Thrasher unit (PG2158) .....	31
4.1.7 Avadlek unit (J01) .....	32
5. Discussion .....	34
5.1 Origin of soil organic matter in surficial permafrost .....	34
5.2 Preservation and degradation of soil organic matter in surficial permafrost .....	36
5.2.1 Surface versus Subsurface conditions .....	37
5.2.2 Mass wasting and stabilised slopes .....	38
5.2.3 Peatland development .....	40
5.2.4 Eco units with heterogenous conditions .....	41
5.3 Possible explanation of biogeochemistry and stable carbon isotope characteristics with the help of environmental statistical tools .....	43
6. Conclusions & Outlook .....	46
7. References .....	48
8. Appendix .....	53
9. Danksagung .....	59

## List of Figures

Fig. 1: Circumpolar permafrost distribution map .....	2
Fig. 2.1: Geographical setting of Herschel Island .....	4
Fig. 2.2: Geological setting of Herschel Island .....	5
Fig. 2.3: Temperature and Precipitation Chart of Herschel Island, Komakuk Beach and Shingle Point .....	7
Fig. 2.4: Typical vegetation communities on Herschel Island .....	8
Fig. 2.5: Classification of underground ice .....	10
Fig. 2.6: Typical morphology on Herschel Island .....	11
Fig. 2.7: Soil spectrum on Herschel Island .....	12
Fig. 2.8: Classification of cryostructure .....	13
Fig. 2.9: Herschel Island ecological unit map .....	14
Fig. 2.10: Coring locations at the southeast part of Herschel Island .....	15
Fig. 3.1: Scheme of working progress for each sample .....	16
Fig. 3.2: Field work .....	17
Fig. 4.1: Summary of moisture content, TOC, TN, C/N atomic ratio and $\delta^{13}\text{C}$ for the Guillemot unit .....	24
Fig. 4.2: Summary of moisture content, TOC, TN, C/N ratio and $\delta^{13}\text{C}$ for the Herschel unit .....	26
Fig. 4.3: Summary of moisture content, TOC, TN, C/N ratio and $\delta^{13}\text{C}$ for PG2155 for the Komakuk unit .....	27
Fig. 4.4: Summary of moisture content, TOC, TN, C/N ratio and $\delta^{13}\text{C}$ for the Orca unit .....	29
Fig. 4.5: Summary of moisture content, TOC, TN, C/N ratio and $\delta^{13}\text{C}$ for the Plover and Jaeger unit .....	31
Fig. 4.6: Summary of moisture content, TOC, TN, C/N ratio and $\delta^{13}\text{C}$ for PG2158 for the Thrasher unit .....	32
Fig. 4.7: Summary of moisture content, TOC, TN, C/N ratio and $\delta^{13}\text{C}$ for the Avadlek unit .....	33
Fig. 5.1: Elemental (atomic C/N ratio) and isotopic ( $\delta^{13}\text{C}$ value) identifiers of bulk organic matter .....	35
Fig. 5.2: Correlation of moisture content and slope gradient with the mean TOC content of each core .....	37

---

Fig. 5.3: Advanced Classification of the coring sites in respect to slope gradient and mean moisture content in active/stabilised .....	39
Fig. 5.4: Schematic diagramm of decay of organic matter in peatlands underlain by permafrost .....	41
Fig. 5.5: PCA ordination diagram of TOC, TN, C/N ratio and $\delta^{13}\text{C}$ response variables .....	45

---

## List of Tables

Tab. 2.2: Summary of key parameters of each eco unit and the according site and drill core information .....	15
Tab. 4.1: Facies description of permafrost layers in PG2152, PG2154 and PG2163 (Herschel unit) .....	25
Tab. 4.2: Facies description of permafrost layers in PG2156, and PG2159 (Orca unit) .....	28
Tab. 4.3: Facies description of active layer in PG2162 (Jaeger unit) .....	30
Tab. 5.1: Observed and calculated eco unit qualities .....	39
Tab. 5.2: Statistical significance of TOC contents between the Guillemot unit (PG2150, PG2151) and the other coring sites .....	40

## Abstract

Organic matter in soils of northern high latitudes show a high lability to recent permafrost thaw. Mobilisation and release of soil organic matter (SOM) in permafrost areas might have a significant impact on the carbon and nitrogen flux into the marine environment and in the atmosphere which motivated scientists in the past to quantify carbon and nitrogen stocks. However, the determination of environmental factors and their influences to SOM storage still need to be investigated more accurately. This thesis seeks to contribute to an improvement of this issue.

This study investigates the SOM in the active layer and surficial permafrost on Herschel Island in the western Canadian Arctic. It evaluates the preservation and degradation status of SOM in relation to different landscape phenomena. To reach this goal, soil moisture, total organic carbon (TOC) and total nitrogen (TN) contents were analysed on 128 samples from twelve sediment cores. The stable carbon isotope ( $\delta^{13}\text{C}$ ) composition on organic carbon and TOC/TN ratios (C/N) were determined. Drilling locations were chosen based on of morphology, vegetation and soil properties and supported by satellite imagery and air photos which classify the surface of Herschel Island into seven ecological units. Regression analyses and principal component analysis (PCA) were used to work out possible correlations and significant differences between environmental factors. Seasonal thaw depths (active layer depths) increase with disturbance and a decreasing vegetation cover and show depths between 20 and 100 cm. Results on organic matter show that consistently well-preserved SOM is accumulated in the active layer and subjacent ice-rich permafrost of depressional polygonal tundra. Waterlogging leads to reduced organic matter decomposition and an enrichment of the TOC and TN content characterising depressional polygonal tundra as a peatland environment. Upland plateaus, gently rolling terrain and alluvial fans represent more than 50 % of the island and show heterogeneous SOM storage characteristics with mostly considerable TOC contents being limited to the active layer. SOM storage in subjacent permafrost is reduced. Disturbed areas with slope gradients greater than  $6^\circ$  show strong SOM degradation with consistently low SOM contents throughout the active layer and permafrost strata. Stabilised slopes show a reestablishment of a vegetation cover and indicate initiation of SOM accumulation. This study highlights the heterogeneity in SOM storage on Herschel Island which is mainly due to local morphology, soil type, vegetation and moisture content. Principal component analysis shows that a gradient of reduced SOM content is evident with increasing ground disturbance. Improved drainage decreases the preservation of SOM in the active layer and ice rich permafrost can hold considerable SOM contents. Future deepening of the active layer with increasing air temperatures in the Arctic might remobilise SOM stored in ice-rich permafrost, especially in peatland environment.

## 1. Introduction

### 1.1 Scientific rationale

The northern high latitudes are characterized as highly vulnerable environment with a sensitive interplay between climate, vegetation and soil conditions. Permafrost is the major occurrent ground phenomenon in the northern high latitudes covering  $22.79 \times 10^6 \text{ km}^2$  or 23.9% of the northern hemisphere land mass (*Zhang et al.*, 1999; Fig. 1). Permafrost or perennially frozen ground is defined as ground (soil or rock including ice or organic material) that remains at or below  $0^\circ\text{C}$  for at least two consecutive years (*Van Everdingen*, 1998). Changes in permafrost distribution are primarily linked to near surface air temperature (*UNEP*, 2012). Permafrost is overlain by seasonally frozen and thawed surface layer called active layer with current depths between 30 and 200 cm (*UNEP*, 2012). The thickness of the active layer varies from year to year depending on controls such as ambient air temperature, slope orientation and angle, vegetation, drainage, snow cover, soil and/or rock type, and water content (*French*, 2007).

In the course of global warming, in the Arctic, the increase in the average surface air temperature will be nearly double the global average (*IPCC*, 2007). In the high latitudes it can lead to 1.) strong northward shifts of the tree line, 2.) increased development of thermokast lakes, 3.) intensified coastal erosion and 4.) increased precipitation which locally raises the snow depth. These processes may have major impact on surficial permafrost distribution in the northern circumpolar region.

The active layer and subjacent cryosols hold considerable amounts of soil organic carbon (SOC). *Tarnocai et al.* (2009) estimates the SOC storage in permafrost with 1672 Pg (1 Pg =  $10^{15}$  g). It represents 50% of the global below ground organic carbon which is more than twice the amount currently in the atmosphere (*Tarnocai et al.*, 2009). Permafrost thaw results in decomposition of organic matter and the release of greenhouse gases ( $\text{CO}_2$  and  $\text{CH}_4$ ) to the atmosphere where it reinforces absorption of solar radiation which is one main factor of global warming. This positive feedback again may accelerate permafrost thaw and can lead to a serious hazard for both local and global habitats for animal and human population.

Research on the terrestrial permafrost carbon pool has increased significantly in the last decade (e.g. *Zimov et al.*, 2006; *Schuur et al.*, 2008; *Kuhry et al.*, 2010). Governmental and non-governmental organisations like the International Permafrost Association (IPA) are engaged in permafrost research to provide valuable qualitative and quantitative output. Projects like the European Union funded "Changing permafrost in the Arctic and its Global Effects in the 21st Century" (PAGE21) or the IPA funded "Global Terrestrial Network for Permafrost" (GTN-P) with his monitoring programmes



"Thermal state of permafrost" (TSP) and circumpolar active layer monitoring network (CALM) improve estimation of the arctic permafrost carbon and nitrogen distribution through detailed field studies and monitoring in order to quantify their size and their vulnerability to climate change.

Above stated examples show that many research programs have a preferential focus on estimation of quantity of the circumpolar carbon pool, but qualitative information on organic matter is still sparse. Herschel Island research history as well lacks on such qualitative characterisation of the organic matter supply where this thesis will hopefully contribute to an respective improvement. Preservation, alteration and degradation of soil organic matter are constant mechanism in the path between deposition (freezing) and remobilisation upon thaw. They eventually control the quantity of carbon release to the atmosphere and needs to be better assessed.

This work has been carried out within the framework of the Helmholtz Young Investigator Group "COPER" (coastal permafrost erosion, organic carbon and nutrient release in the arctic nearshore zone) located at the Alfred Wegener Institute Potsdam, a scientific programme assessing the pace and nature of sediment and organic matter transfer into the southern Canadian Beaufort Sea with regard coastal erosion and thermokarst processes.



**Figure 1** Circumpolar permafrost distribution map. Red circle marks the study area (Brown et al. 1998, modified)

## **1.2 Aims and objectives**

This thesis shall contribute to improve the understanding of formation, alteration and degradation of the organic matter in near-surface permafrost on Herschel Island. To reach this goal biogeochemical analyses as well as stable carbon isotope determination were combined with geological background information from previous studies and statistical analysis. Five core objectives will be worked out in the course of this thesis:

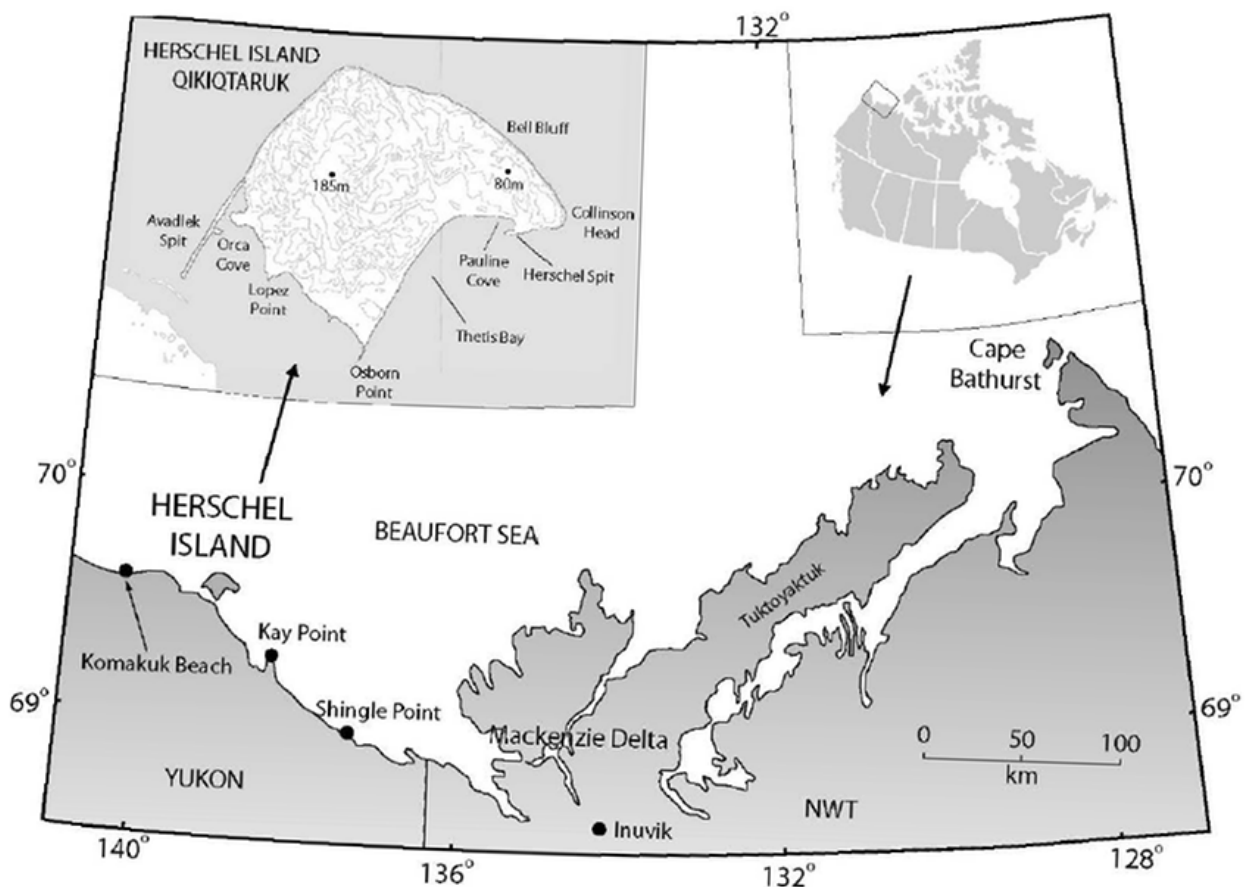
- To quantify moisture content, total organic carbon, total nitrogen and stable carbon isotope in different ecological units
- To determine the origin of soil organic matter incorporated in the different ecological units
- To show which soil condition and morphology phenomena favour preservation or degradation of soil organic matter
- To work out the differences in soil organic matter characteristics between active layer and subjacent permafrost
- To find environmental parameters that can explain biogeochemistry and stable carbon isotope characteristics

## 2. Study area

### 2.1 Geographical setting and geological background

#### *Geographical setting*

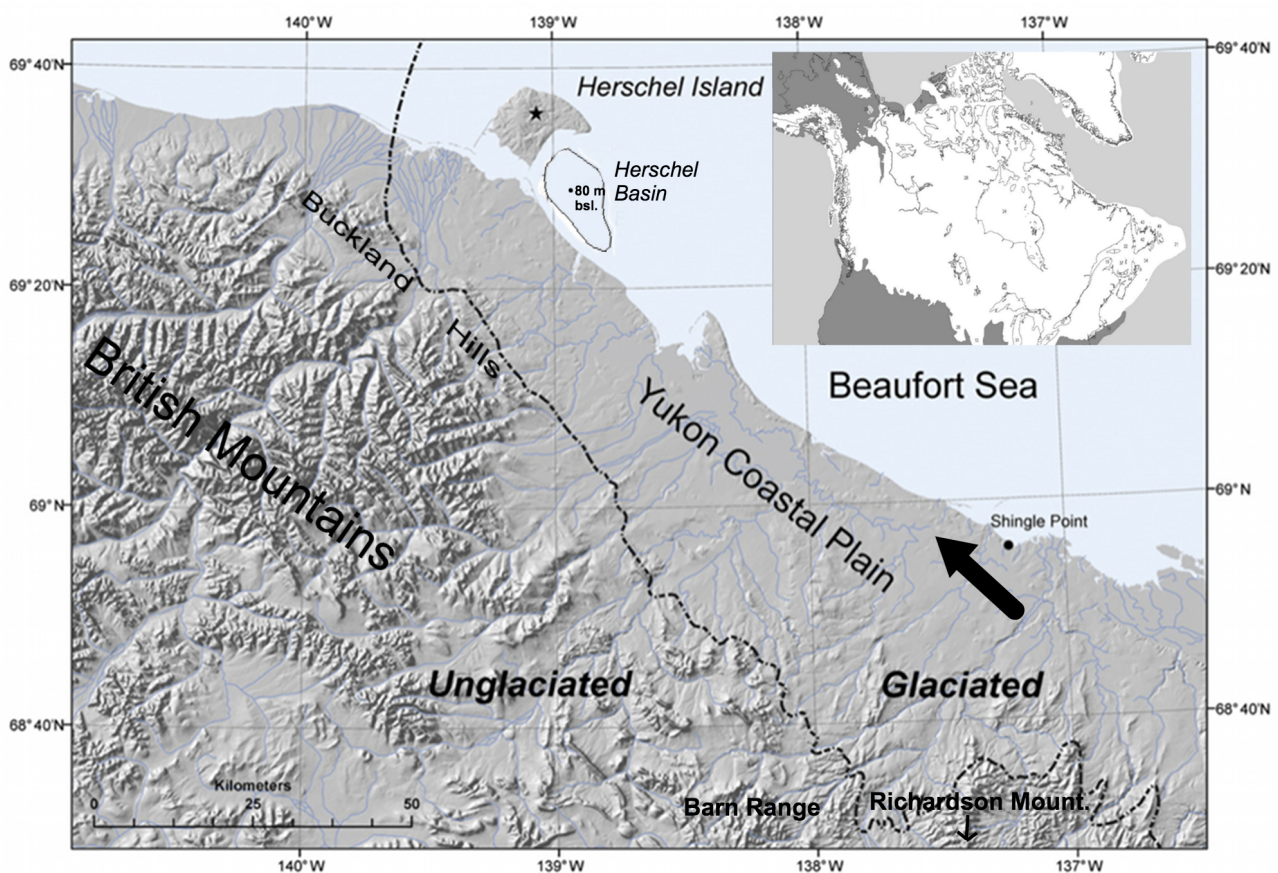
Herschel Island ( $69^{\circ}36'N$ ,  $139^{\circ}4'W$ ) is the northernmost point of the Yukon Territory and is located in the southern Beaufort Sea. It lies 3 km offshore from the Yukon coast, 60 km east of the Alaska-Yukon border and 200 km west of Inuvik as the nearest larger settlement. The Island covers an area of 108 km<sup>2</sup> and has a maximum elevation of 185 m asl (*Lantuit, 2005*) which rises near to the center of the island (Fig. 2.1).



**Figure 2.1** Geographical setting of Herschel Island (*Lantuit, 2005*; modified by *Fritz, 2008*)

### Geological background

According to *Rampton* (1982) Herschel Island is part of the Yukon Coastal Plain (YCP) physiographic region. The YCP is approximately 200 km long and 10 to 60 km wide (*Lenz*, 2010 Fig. 2.2). Its basement is a tertiary pediment, which gently slopes northwest of the British, Barn and Richardson mountains and the Buckland Hills. During the Last Glacial Maximum (LGM) in the late Wisconsin (19 - 22 cal ka BP; *Dyke et al.* 2002) the Laurentide Ice Sheet (LIS) advanced onto the YCP, where it reached its westernmost position slightly west of Herschel Island (Fig. 2.2). The LIS ice lobe ploughed up mixed deposits of generally marine, littoral and terrestrial characteristics (*Bouchard*, 1974) from the current Herschel Basin to form a push moraine now called Herschel Island. The volume of sediment missing at Herschel Basin roughly corresponds to the volume of Herschel Island (*Mackay*, 1959; Fig. 2.2).



**Figure 2.2** Geological setting of Herschel Island. Dashed line marks the boundary of the glaciation phase, arrow shows advance direction (*Lenz*, 2013, modified). Small window shows maximum glaciation in North America during Last Glacial Maximum (*Dyke et al.*, 2002, modified)

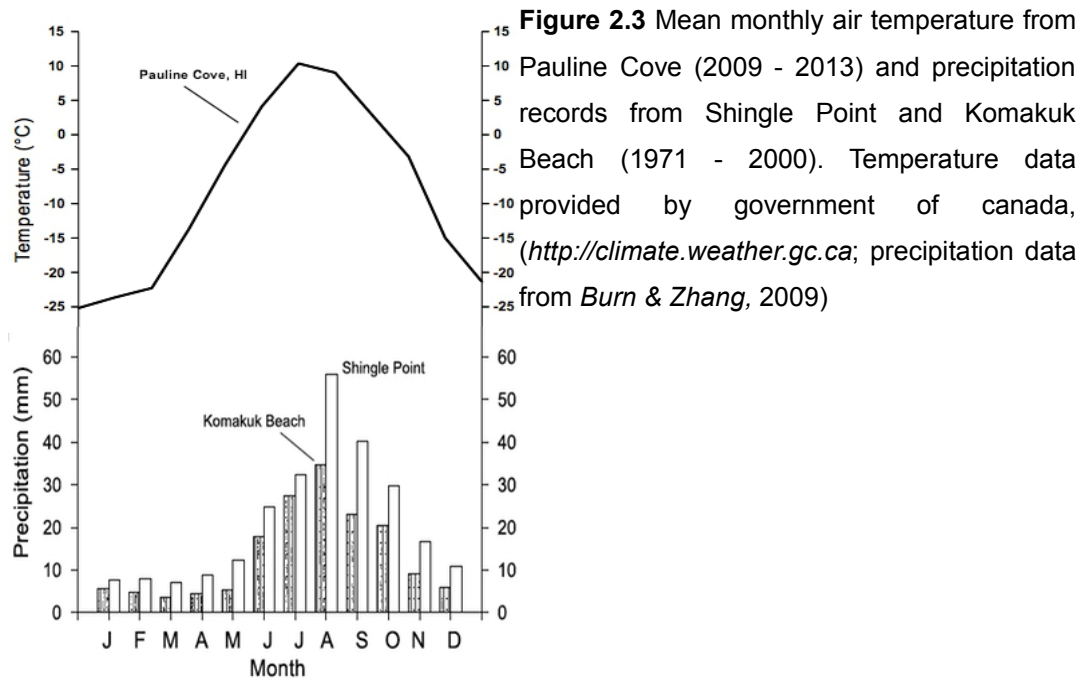
In the early Holocene (~12 to 10 cal ka BP) a precession driven summer insolation maximum, in combination with the waning LIS (*Kaufmann et al.* 2004) caused a rapidly transgression sea from

its regional minimum of ~140 m below present (*Hill et al.* 1985) toward approximately modern sea level. In combination with rising summer temperatures (*Burn et al.* 1997) the sea level rise would have delivered more moisture to a formerly continental area that evolved into a coastal maritime environment (*Kaufman et al.*, 2004). In this so called Holocene Thermal Maximum (HTM) warmer and wetter conditions than today supported a vegetation shift, extensive thermokarst, peatland development and a deepening of the active layer to as much as 1.5 to 3 m below the modern surface on Herschel Island (*Fritz et al.*, 2012). The middle Holocene promoted a cooler and wetter climate, leading to ice-wedge growth, permafrost aggradation, thawlake drainage and paludification (*Ritchie*, 1984; *Mackay*, 1992; *Cwynar and Spear*, 1995; *Eisner et al.*, 2003). Coastal erosion and retrogressive thaw slump (RTS) activity occur since sea level stabilisation and lead to intense retreat of Herschel Island coastlines.

## 2.2 Climate and vegetation

### *Climate*

According to the *Koepfen-Geiger* (1884, translated 2011) classification Herschel Island owns a polar tundra climate (Koeppen-Geider code: ET). Temperatures rise above 0°C only during summer months (June - September) and have a maximum at around 10 °C. During winter months (October - May) the temperatures decrease to a minimum of -25 °C. The annual mean temperature averages -8.5 °C. The climate is more continental affected due to a thick ice cover on the Beaufort Sea which remains ice free only during summer months. Annual precipitation is also affected by ice cover. More than 70% of annual precipitation occurs along the ice free season mainly as rain (*Burn & Zhang*, 2009). There are two major wind directions. Prevailing wind from the northwest lashes most of the time but during the open water season wind approaches the coast from east and induces strong coastal slump retreats. Because of its remote setting continuous data records for temperature and precipitation is still missing and through 1995 the closest weather stations were onshore at Komakuk Beach and Shingle Point (see Fig 2.1). Since 1995 a weather station (temperature records only) is operating at Pauline Cove on the southeastern coastline of Herschel Island. Data records are provided by the government of Canada and can accessed under <http://climate.weather.gc.ca/>.



### Vegetation

Herschel Island inland vegetation is ruled by cold and harsh climate. Persistent wind, annual mean Temperature of  $-8^{\circ}\text{C}$  and a marginal water supply due to low precipitation rates confine the growth of plants so that low height tundra vegetation with herbs, shrubs, grasses, mosses and lichens is prevalent. The coastal areas differ due to lower elevation and influence of sea water temperature and nutrient content. *Smith et al.* (1989) categorised local vegetation phenomenon. As a result he classified 194 plant species of 28 families in 11 vegetation types.

Sedges (*Carex*, *Eriophorum Sp.*), grasses (*Tussock*), moss (*Bryophytes*), arctic willow (*Salix arctica*) and dryas-vetch (*Astragalus*) are the most common occurent plants and widespread both on uplands and valleys. Vegetation cover is linked to slope gradient meaning that occurrence of bare ground increases potentially with this parameter.



**Figure 2.4** Typical vegetation communities on Herschel Island. A: cottongrass meadow; B: *Salix-Arctica* (green leaves) and Vetches (*Astragalus*, purple colored). (Photos: M. Fritz, 2013)

### 2.3 Periglacial processes, geomorphology and soil development

#### *Periglacial environment*

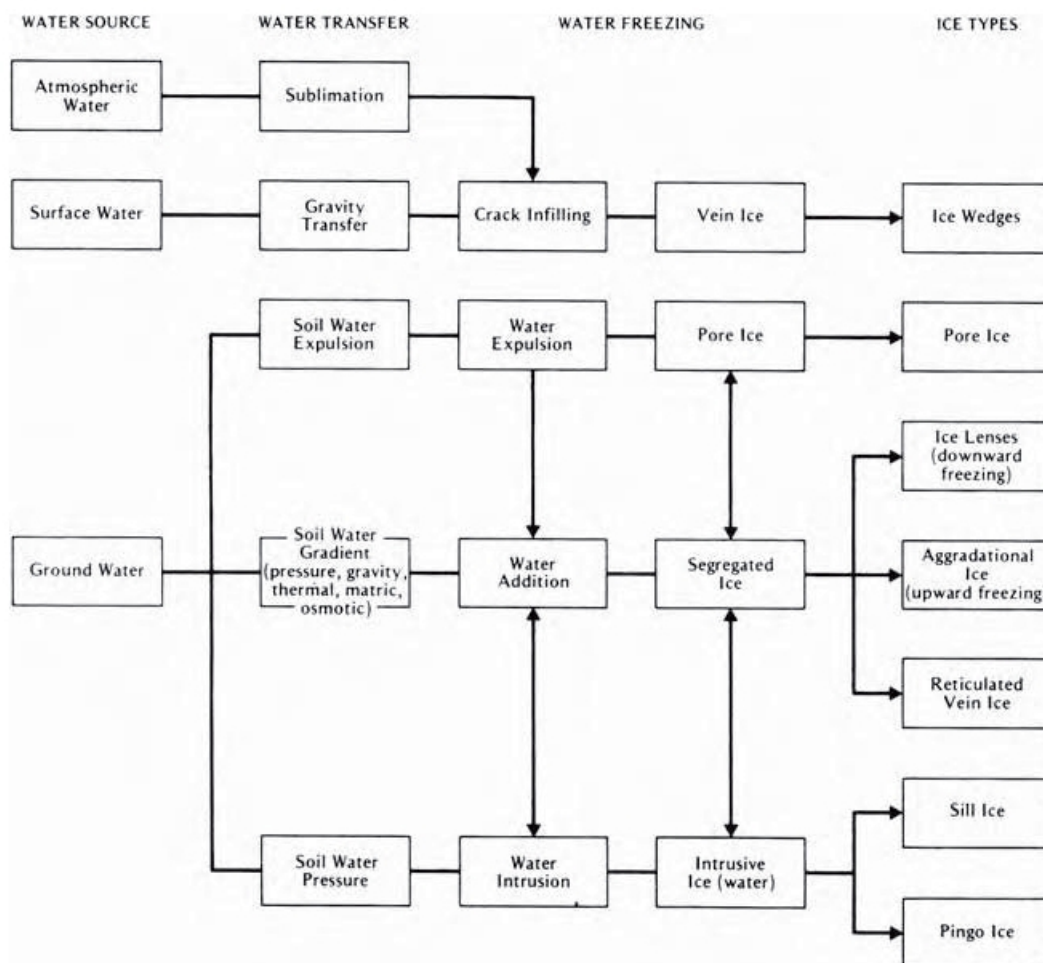
The geomorphology and soil development on Herschel Island are strongly linked to periglacial processes. Processes that are unique to periglacial environment relate to ground frost action (French, 2007) which is strongly linked to the ground temperature. Factors that influence mostly the thermal state of the ground are air temperature and snow thickness and vegetation cover. V. J. Lunardini (1991) outlined these parameters to the n-factor which describe roughly a transfer function between air and ground surface temperature due to the heat flux conducted to the ground generated by emissivity of vegetation, bare ground or snow cover through incoming solar radiation. For more details see Lunardini (1991, pp. 437). Generally, freezing begins during the phase change of liquid water into solid water. The freezing point of pure water is at 0°C but salinity due to different soil chemistry can lower this point. The phase transition leads to a volume increase by 9% which has important consequences for cryogenic processes. Permafrost is also defined on the basis of temperature, to be more specific, ground that remains at or below 0°C for at least two consecutive years (Van Everdingen, 1998). Permafrost distribution can be differentiated in continuous, discontinuous and sporadic and isolated permafrost (Brown *et al.*, 1998; Fig. 1). Herschel Island lies in the continuous permafrost zone meaning more than 90% of the ground is perennially frozen.

Besides, due to recently rising temperatures, the role of the active layer increases significantly. In the continuous permafrost zone, the active layer lies between the ground surface and the permafrost table. Primary triggered by higher susceptibility to air temperature, ground temperature rises above

0°C and freeze-thaw action happens here on a seasonal or even diurnal basis. The active layer depth varies on Herschel Island between 15 and 100 cm.

The quality and quantity of ice growth depends on moisture supply, soil properties, freezing process and duration of the frozen stage (*French, 2007*) and can be classified into four categories of ground ice (Fig. 2.5). With reference to Herschel Island segregated ice, pore ice and vein ice dominate. Segregated ice generally occurs in permafrost with prevalent particle size  $<0,01\text{mm}$  (*French, 2007*) inducing high capillarity. It leads to a water table rise towards the freezing plane where it aggrades with lateral orientation into ice lenses. Volume increase during the segregation induces frost heave due to pressure on overlying ice and soil. Pore ice occurs more in coarse grained soil where capillarity is low and water freezes interstitially. It results in ice growth without preferential orientation. Vein ice is formed by the penetration of water (e.g. meltwater) into open fissures of the ground surface (*French, 2007*). Fissures are generated by thermal contraction cracking, a typical phenomenon of mechanical weathering. In summer surface water fills the fissure and freezes instantaneously due to negative ground temperature. In ensuing year additional surface water reaches the fissure and lets them further grow. Repeated frost cracking can add several ice veins resulting in the formation of ice wedges in the ground and typical polygonal networks at the surface. Ice wedges are classified in epigenetic (lateral growing in pre-existing permafrost), syngenetic (upward growing with surface aggradation) and anti-syngenetic ice wedges (growing with depth, i.e. where erosion occurs).





**Figure 2.5** Classification of underground ice. (adapted from Mackay, 1972, modified)

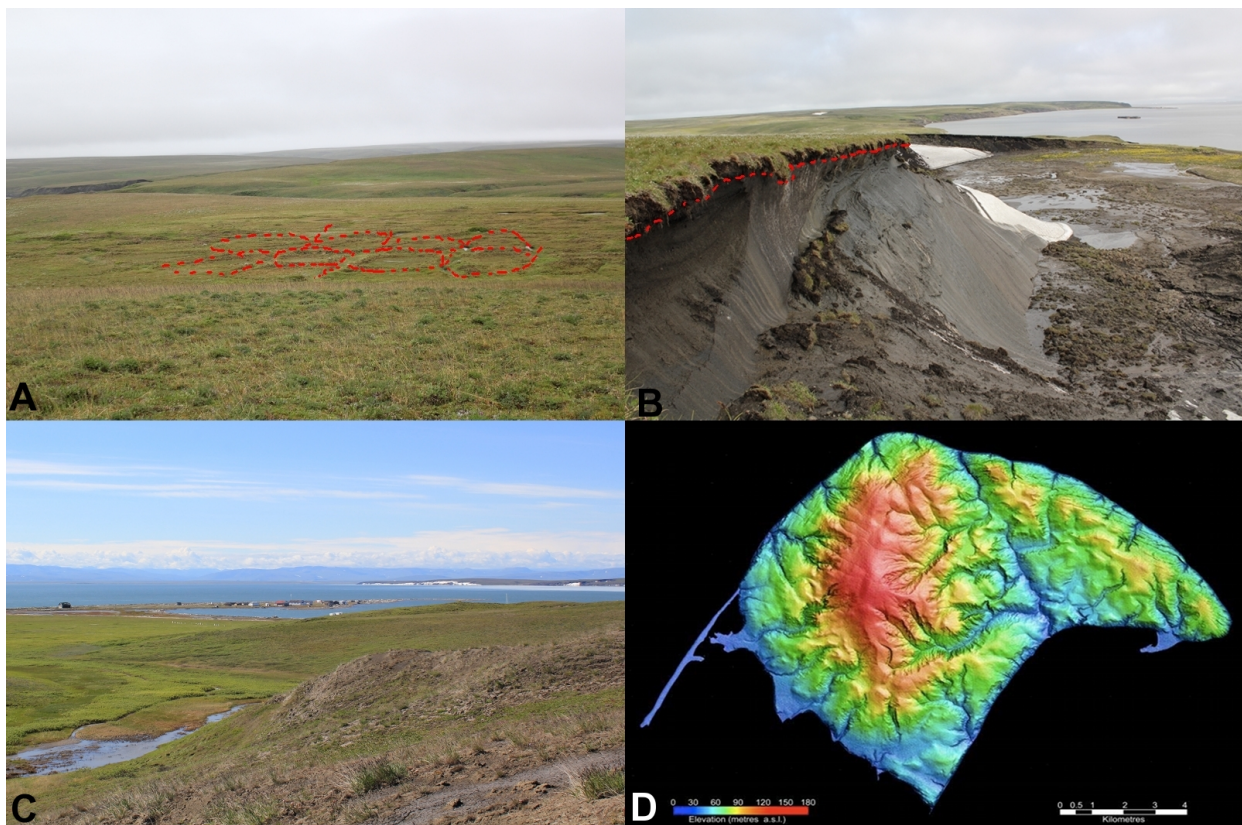
### Geomorphology

The previous chapter introduced that cold temperatures arouse frost action and furthermore thermal contraction cracking. In conjunction with moisture apply, different ground ice forms induces frost heaving. Freeze-thaw action induces thermokarst subsidence, and in conjunction with slopy terrain it induces thermal erosion resulting in mass movement with sustainable effect on soil development which to be discussed in the following.

The dominant morphology on Herschel Island are undulation uplands, rolling hills and ridges + valleys (>50% of total terrain) confined by depressional polygonal ground. It owes its landscape from glacial ice thrust, which deposited moraines and postglacial overprint such as thermokarst activity and polygon development. (Rampton, 1982). Thermokarst describes thaw subsidence due to melt out and drainage of excess ground ice (e.g. ice wedge, pore ice). The generally rolling terrain is caused by those kind of periglacial feature (Fig. 6A). Depressional polygonal tundra due to ice wedge cracking is located in areas of imperfect to poor drainage. Those ice-wedge polygon can either have a low and wet center (low-centered polygons) with elevated rims or high centers (high-

centered polygons) with water-filled through above already degrading ice wedge. Several circles and polygons are placed side by side to form patterned ground which are characteristic for arctic tundra as it can be observed on upland plateaus as well as depressional ground on Herschel Island (Fig. 6A).

The island is drained from uplands east and west of the Island (Fig 6D). Alluvial fans and fluvial streams run off via gullies to the coast. Gully appearance refers to thermal erosion processes, where surface runoff from snowmelt, summer precipitation or thawing permafrost becomes concentrated along zones of weakness, causing preferential thaw (*French, 2007, Fig. 6C*). The saturated active layer becomes unstable and gravity related mass movement such as solifluction and frost creep apply. In addition, underlying permafrost table may act as a slipping plane and supports gelifluction. While the interior of Herschel Island shows a more hummocky topography the coastline, especially the southeastern part, is characterised by strong retrogressive thaw slump activity and active layer detachment slides (*Lantuit, 2005; Fig. 6B*). The coastline morphology varies from steep bluffs up to 60 m high (*Burn & Zhang, 2009*) to gentle slopes with spits and sandy beaches.

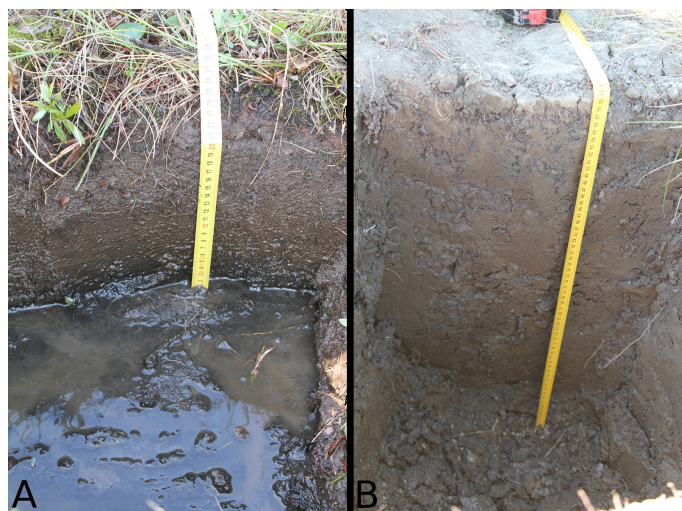


**Figure 2.6** Typical morphology on Herschel Island. A: Hummocky terrain with polygonal ground (red dashes mark polygons edges) . B: Coastal bluff with strong retrogressive thaw slump retreat (dashed line mark active layer limit). C: erosive surface induced by solifluction and gully erosion. D: Digital elevation model of Herschel Island (Photos: M. Fritz, 2013; elevation model from IKONOS data 2004, Natural Resources Canada, Canada Centre for Remote Sensing)

### *Soil development*

Cryosols (gelisols) are restricted to permafrost occurrence where three soil types can be subdivided: 1.) turbic cryosol, 2.) static cryosol and 3.) organic cryosol (*Canadian Soil Classification System*). While the latter is generally more occurring in uncontinuous and sporadic permafrost (*Tarnocai et al., 2009; Harden et al., 2012*), the first two are widespread on Herschel Island and its distribution is linked to local morphology. Sediments are generally, fine grained (clay, silty loam) with occasional sand and gravel content due to its marine to littoral background (*Rampton, 1982*). Only at beaches and spits, more coarse material (gravelly sand, pebbles) occurs.

Turbic cryosols show strong cryoturbation caused by deep frost action and frost heave. Ice wedges and segregated ice development in combination with imperfect to poor drainage leads to material displacement, sorting and broken to mixed horizons (*French 2007; Smith, 2007*). Active layer depth averages 20 - 30 cm. Depressional polygonal tundra underlaid by this soil type. If water is permanently present then gleysolic turbic cryosol is the prevalent soil type (Fig. 7A). As slope gradient increases, cryoturbation loses influences and erosion as well as mass movement becomes more important. This leads to improved drainage and prohibit the development of a B horizon. The active layer deepens up to 100 cm. A transition from turbic to static cryosol becomes distinct (Fig. 2.7B). Furthermore, frost action develops different kinds of cryostructures. They are helpful to assess distinct changes, moisture supply and depositional conditions. The determination of the maximum active layer depth is contributed by changes in cryostructure. Figure 2.8 summarises important cryostructures and link them with sediment and ice type.



**Figure 2.7** Soil spectrum on Herschel Island. A: Orthic turbic cryosol. B: Static cryosol. (Photos: M. Fritz, 2013)

(A)

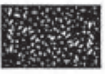





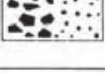
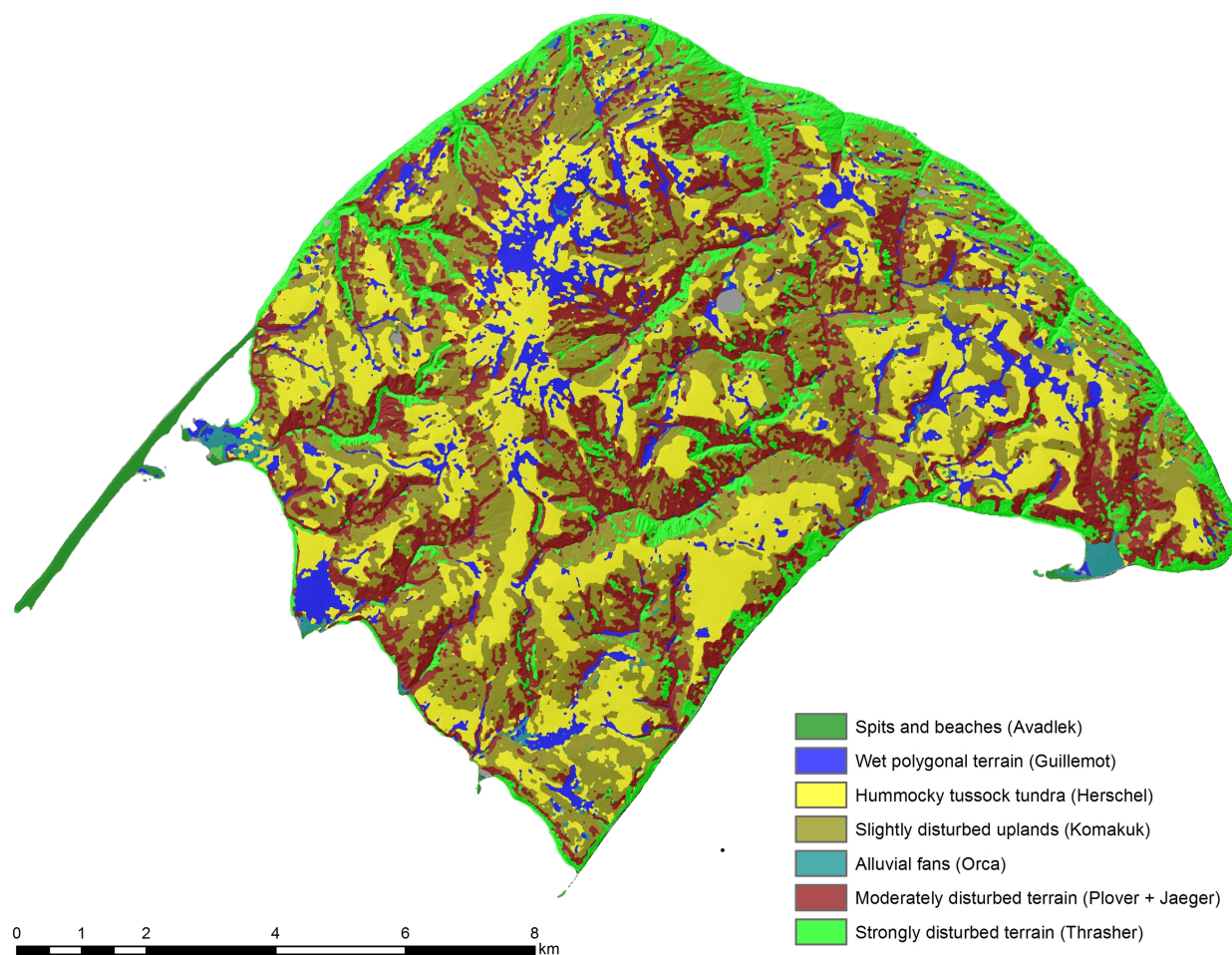
CRYOSTRUCTURE AND CODE	SEDIMENT	ICE	OCCURRENCE AS OR WITHIN			
 structureless (Si)	sand gravel	pore	ice in sand + gravel			
 lenticular (Le)	muddy peat mud (fine sand)	sand	segregated	crack infill	ice/sediment lenses massive ice icy sediments	(ice wedges) (composite sand-ice wedges) (dilation-crack ice)
 layered (La)	muddy peat mud (fine sand)	sand	segregated intrusive	crack infill	ice/sediment layers massive ice icy sediments	ice wedges composite sand-ice wedges dilation-crack ice
 regular reticulate (Rr)	mud		segregated		ice in mud	
 irregular reticulate (Ri)	mud		segregated		ice in mud	
 crustal (Cr)	mud frost-susceptible clasts		segregated			
 suspended (Su)	mud sand gravel	mud sand gravel	segregated intrusive		icy layer at top of permafrost ice dykes in mud	ice lenses massive ice icy sediments ice dykes

Figure 2.8 Classification of cryostructure proposed by Murton and French (1994)

### 2.4 Ecological unit distribution

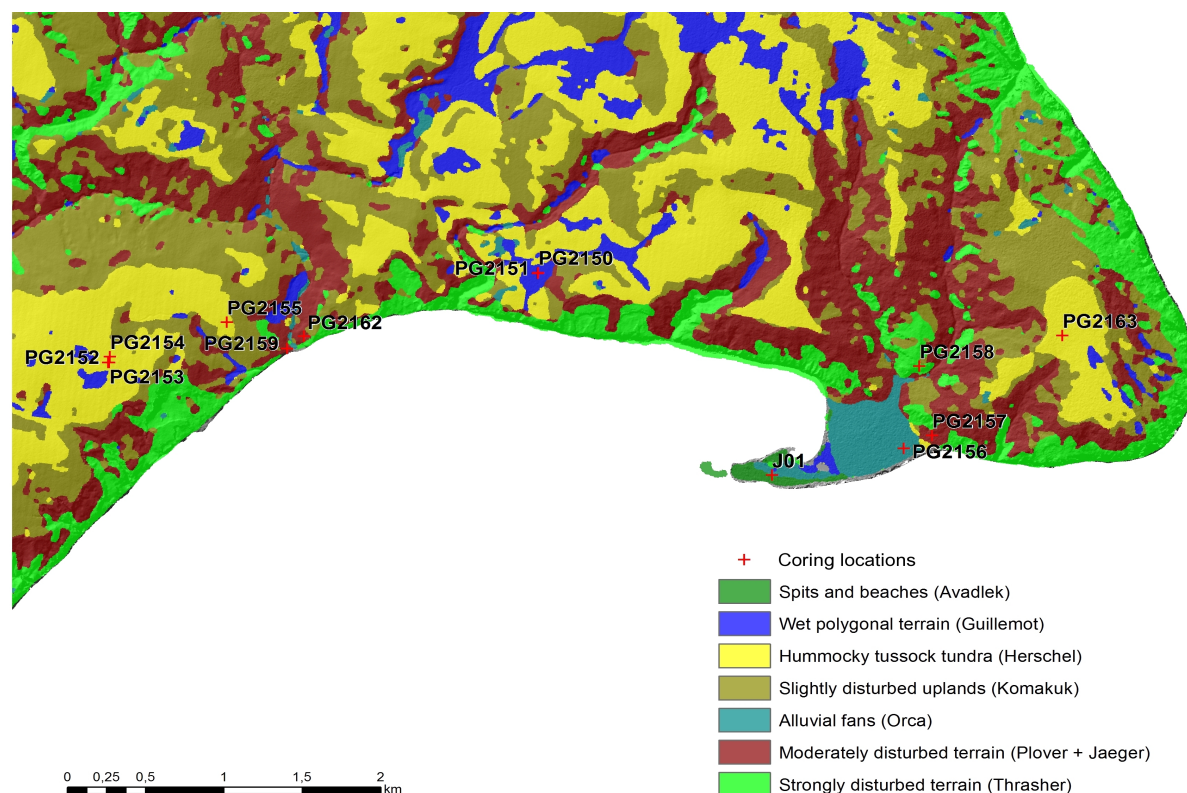
Based on the previous information about morphology, vegetation cover and soil development, Herschel Island surface area was assessed and partitioned into eight ecological units first developed by Wicken *et al.* (1981) and enhanced by Smith *et al.* (1989). These simple, recurrent properties and map labels allow the transfer of knowledge from a familiar area to an unfamiliar area elsewhere on the map (Smith *et al.*, 1989). The actuality of partitioning in now seven units (Plover and Jaeger were summarized due to distinct features; Fig. 2.9) is still given. However, modern remote sensing facilities like satellite imagery and software supported georeferencing offer much higher resolution which improve the assignment of particular units. In August 2010, a RapidEye satellite image of Herschel Island was taken with horizontal resolution of 6.5 m. This image was georeferenced on the basis of ground control points taken in the field and orthorectified with a digital elevation model (DEM) (Obu *et al.*, unpublished).



**Figure 2.9** Herschel Island ecological unit map based on satellite imagery and georeferencing (Image: *Obu et al.*, unpublished)

## 2.5 Sites description

Coring locations were selected according to the pre-defined ecological units, accessibility and were supposed to cover all units. Twelve cores were drilled in summer 2013 along the southeast part of Herschel Island at the eastshore around Pauline Cove (Fig. 2.10). At least one core from each unit was obtained. Table 2.1 summarises morphology, vegetation cover and soil development for each ecological unit. At the coring locations information such as core depth, elevation, slope gradient, exposed soil percentage as well as observed and maximum active layer depth were added. These parameters are available predictors for the organic matter supply.



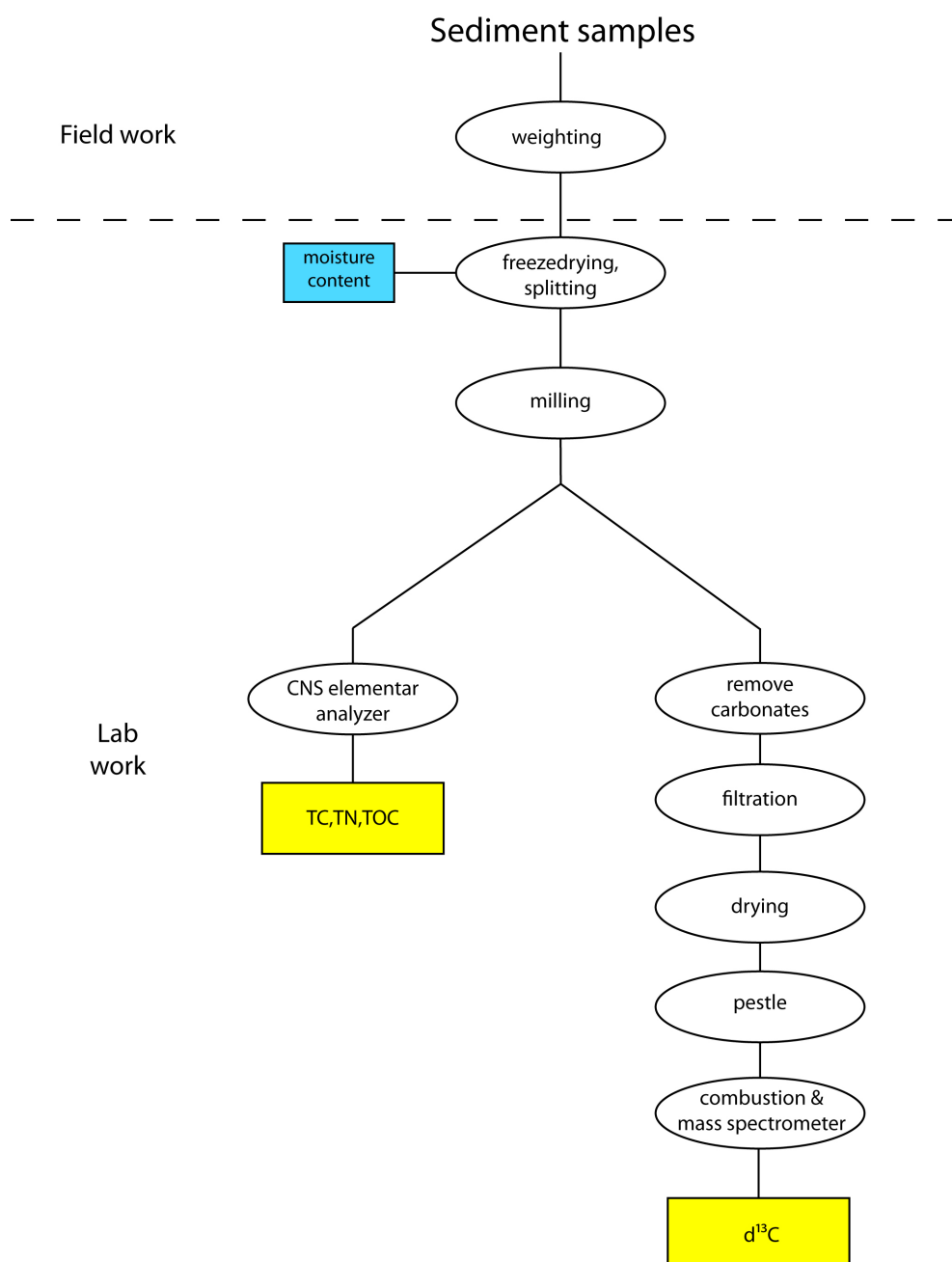
**Figure 2.10** Coring locations at the southeast part of Herschel Island. Sites are tagged with a red cross and labeled with core numbers and unit name. (Image: *Obu et al.*, unpublished)

**Table 2.1** Summary of key parameters of each eco unit and the according site and drill core information. Note that maximum active layer depth for PG2162 and J01 could not be determined because either water filled the pit (J01) or gravel occurrence stopped drilling (PG2162). (adapted from *Smith et al.*, 1989, modified)

Unit	Terrain Feature			Core Site Information							Soil	Vegetation
Name	Approx. Extent (% of Herschel Island)	Topography/Landform	Gully Erosion	Core Nr.	Core Depth (cm)	Elevation (m asl)	Slope (°)	Exposed Soil (%)	Observed Active Layer Depth (cm)	Maximum Active Layer Depth (cm)	Soil Development	Vegetation Cover
Guillemot (Gu)	4	wet polygonal terrain	none	PG2150	218	26	0	0	15	27	Gleysolic Turbic Cryosol	Cottongrass/Moss
				PG2151	250	23	0	10	31	63		
				PG2152	63	57	2	0	34	49		
Herschel (He)	15	hummocky tundra	none	PG2154	198	57	2	0	18	19	Orthic Turbic Cryosol	Cottongrass/Moss
				PG2163	230	93	4	0	33	46		
Komakuk (Ko)	44	slightly disturbed uplands	slight	PG2155	197	32	1	0	31	52	Orthic Turbic Cryosol	Arctic Willow/Dryas-Vetch
Orca (Or)	1	alluvial fans	depositional	PG2156	227	5	1	0	49	60	Regosolic Static Cryosol	Sedge Grass/ Moss
				PG2159	200	2	5	3	28	43		
Plover+Jaeger (Pl+Ja)	23	moderately disturbed terrain	slight – moderate	PG2157	190	15	7	20	46	67	Regosolic Turbic Cryosol	Arctic Willow/Dryas-Vetch/Saxifrage-Coltsfoot
				PG2162	70	40	8	5	70	NA		
Thrasher (Th)	13	strongly disturbed terrain	severe	PG2158	143	50	9	80	77	98	Regosolic Static Cryosol	Carex/Salix
Avadlek (AV)	1	splits and beaches	marine erosion and deposition	J01	40	1	0	2	>50	NA	Regosolic Static Cryosol	Wild Rye

### 3. Methods

This chapter describes the process to obtain accurate data by running through sample taking, preparation and finally, machine analysis. It is subdivided in field work and laboratory work and comprise the handling of 128 samples distributed on 12 sediment cores. Fig. 13 illustrates the structure of this working process. Besides instrumental analysis, statistical methods will be used to accompany significant differences in the organic matter characteristics and assign environmental parameters to biogeochemistry and stable carbon isotope distribution.



**Figure 3.1** Flowchart of sample treatment

### 3.1 Field work

The drilling and sampling was performed by AWI in the course of expedition Yukon Coast in Juli/August 2013.

A 5x5 m plot was set up at the coring location where vegetation communities and geomorphological parameter were described. The active layer was measured in thickness and described in her lithological characteristics. Samples were taken on a 7.5 x 7.5 cm square with 5 cm thickness equals sample volume of 281 cm<sup>3</sup>. The sample resolution accounted 10 cm. Permafrost were drilled with a SIPRE permafrost drill equipped qith a STIHL BT121 engine with 7.5 cm core diameter. Sampling resolution within first meter below surface was 10 cm and continued with 20cm below one meter. Sample thickness of 5 cm increments was kept unchanged and equals a sample volume of 220 cm<sup>3</sup>. Samples were stored in whirl-pak bags and subsequently thawed and weighed. In preparation of all upcoming analyses, freeze-drying is generally preferred because either air-drying or oven-drying may result in loss of volatile organic matter components, which can bias elemental and isotopic compositions (*Meyers, 2001*)



**Figure 3.2** Field work: Left: Drilling of a permafrost core in cottongrass tussock tundra (PG2154). Right: Core arrangement for sampling and description (PG2156) (Photos: M.Fritz)

### 3.2 Laboratory work

The laboratory work was performed partly in November/December 2013 during an internship at the AWI Potsdam.



### 3.2.1 Moisture content

Soil moisture is derived either from summer precipitation or snow melt and, subject to slope and soil type, it reflects recent drainage conditions. Furthermore, moisture content is an important agent for plant growth, accumulation or degradation of organic matter.

Wet samples were weighed and freeze-dried for at least 2 days and weighed afterwards. The moisture content was calculated by following equation.

$$\text{Moisture Content [\%]} = \left[ 1 - \left( \frac{\text{dry sample weight}}{\text{wet sample weight}} \right) \right] \times 100 \quad \text{Eq. 1}$$

### 3.2.2 Element analysis: TC, TN, TOC

Terrestrial and marine sediments host the depositional environment for plants and algae. Environmental factors such as temperature, precipitation and local morphology control bioproductivity, accumulation and decomposition, leading to differentiated residual carbon and nutrient values, which can be utilised to reconstruct paleoenvironmental condition.

The contents of total carbon (TC) and total nitrogen (TN) in the sediment samples were measured quantitatively with a CNS elemental analyzer (Elementar vario EL III). The principle of measurement is based on catalytic tube combustion by means of oxygen supply at high temperatures (>900°C) (HANDBOOK ELEMENTAR VARIO EL III, 2001). To gain representative analytical results a subsample of about 5 g was grinded and thereby homogenised with the help of a planetary mill (Fritsch) at 3600 RPM. For each sample a weight of 5 mg respectively 8mg was encapsulated in tin capsules twice and released to the analyzer via sample disposer. During combustion in a high oxygen environment, the elements C, H, N and S are oxidised explosively into the gaseous phases CO<sub>2</sub>, H<sub>2</sub>O, NO<sub>x</sub>, SO<sub>2</sub>, SO<sub>3</sub> and molecular N<sub>2</sub>. Copper oxide serves as catalyst for the reduction of nitrous oxide (NO<sub>x</sub>) to N<sub>2</sub>, while a lead chromate fill absorbs SO<sub>2</sub> and SO<sub>3</sub>. Helium (He) serves as carrier gas for the remaining components CO<sub>2</sub>, H<sub>2</sub>O and N<sub>2</sub>. Specific adsorption columns separate the distinctive components that are subsequently detected by a thermal conductivity detector (HANDBOOK ELEMENTAR VARIO EL III, 2001). Finally, the percentage share of carbon and nitrogen is calculated from its absolute gravimetric content compared to the input sample weight.

The contents of total organic carbon (TOC) were measured with a different elemental analyzer (vario MAX C). The principle of measurement is basically the same but combustion takes place on

lower temperatures (~550°C). The required sample weight is based on the TC value and was calculated with the help of an empirical formula.

Carbon/Nitrogen ratios may be used to distinguish between algae and land plants as well as to assess rates of mineralisation during alteration of organic compounds. C/N ratios were expressed in atomic ratio. Obtained C/N ratios were multiplied by 1.167 which is the ratio of atomic weight of nitrogen (<sup>15</sup>N) and carbon (<sup>13</sup>C) (Meyer, 2001).

### 3.2.3 Stable carbon isotopes

Carbon isotopic ratios are useful to distinguish between marine and continental plant source of sedimentary organic matter. During organic matter formation carbon isotopes (<sup>12</sup>C and <sup>13</sup>C) are assembled in distinct ratios and therefore reflect the dynamics of carbon assimilation during photosynthesis and the isotopic compositions of the carbon source (Hayes, 1993). The ratio of carbon isotopes in a given sample is usually stated by the ratio of <sup>13</sup>C to <sup>12</sup>C atoms, reported as ‰-difference against the international reference standard (Vienna Pee Dee Belemnite), expressed as δ<sup>13</sup>C (Craig, 1953; Dansgaard, 1953).

$$\delta^{13}\text{C}[\text{‰}] = \left[ \frac{\left(\frac{^{13}\text{C}}{^{12}\text{C}}\right)_{\text{Sample}}}{\left(\frac{^{13}\text{C}}{^{12}\text{C}}\right)_{\text{Standard (VPDB)}}} - 1 \right] \times 1000 \quad \text{Eq. 2}$$

Most photosynthetic plants incorporate carbon into organic matter using the C<sub>3</sub> Calvin Pathway which biochemically discriminates against <sup>13</sup>C to produce a δ<sup>13</sup>C shift of about -20‰ (Meyers, 1997). Freshwater algae utilize dissolved CO<sub>2</sub> derived from atmospheric CO<sub>2</sub> (δ<sup>13</sup>C ~ -7‰) and give average values of -27‰ (Nakai, 1972). Marine organic matter typically has δ<sup>13</sup>C values between -20 and -22‰ due to incorporate dissolved bicarbonate (Meyers, 1994).

The determination of the stable carbon isotope composition was carried out with a combination of an elemental analyzer (Flash EA 1112 Series, Thermo Finnigan), a CONFLO III gas mixing system and a Thermo Finnigan MAT Delta-S mass spectrometer. Inorganic carbon has the potential to disturb the signal of the biotic source by an Überhöhung of the δ<sup>13</sup>C value. To avoid that disturbance it was necessary to prepare the samples. To retreat carbonate from the samples the following procedure was executed.

- 1) 5 g subsample in 250 ml narrow-necked Erlenmeyer flask were filled up with 1.3 mol hydrochloric acid and was heated for three hours at 97°C

- 2) Dilution with deionised water until ph-neutralisation was achieved
- 3) Solution was vacuum-filtrated and a filter cake was obtained
- 4) Finally, filter cake was dried overnight and homogenised with a pestle

The calculated sample weight ( $m \text{ [g]} = 45 / \text{TOC [\%]}$ ) was encapsulated in tin capsules and released to the analyzer via autosampler system. Measuring control standards and performing repeated determination after every seventh measurement ensures correct analytical values. The Principle of operation for the elementar analyzer was explained in chapter 3.2.2. The produced  $\text{CO}_2$  gas was injected to the mass spectrometer via the CONFLO III gas mixing system and a capillary. An ion source charges the  $\text{CO}_2$  gas and focuses it into a single beam. Afterwards, the single beam was accelerated towards a magnet where the gaseous ion was deflected according to the mass/charge ratio and an electrical current was released and detected. Measurements at AWI Potsdam are reproducible with an accuracy generally better than  $\pm 0.15 \%$ .

### 3.3 Statistical analysis

#### 3.3.1 Regression analysis

Linear regressions are helpful to show the strength of relation between two environmental variables. the mathematical principal is based on the methodic of least squares (*Leyer et al., 2008*). A calculated line through a scatter-plot of a bivariable comparison represents best the occurent relation when the sum of distances between the observed y-value and a calculated  $\hat{y}$ -value is minimum.

$$RSS = \sum_{i=1}^n (y_i - \hat{y}_i)^2 \quad \text{Eq. 3}$$

where RSS is the sum of least squares,  $y_i$  is the observed value and  $\hat{y}_i$  is the calculated value by following linear equation:

$$y_i = bx_i + a \quad \text{Eq. 4}$$

with

$$a = \bar{y} - b\bar{x}, \quad b = \frac{\sum_{i=1}^n (y_i - \bar{y})(x_i - \bar{x})}{\sum_{i=1}^n (x_i - \bar{x})^2} \quad \text{Eq. 5}$$

where  $\bar{x}, \bar{y}$  are the mean of each sample-set. B represents the regression coefficient and give evidence about the ratio and the positive or negative relation between the two environmental variables.

The coefficient of determination ( $r^2$ ) where used to obtain evidence about the strength of correlation in a percentaged value an will be calculated as follows:

$$r^2 = \frac{\sum_{i=1}^n (y_i - \bar{y}_i)^2}{\sum_{i=1}^n (\hat{y}_i - \bar{y}_i)^2} \quad \text{Eq. 6}$$

Obtained values lie in a range between zero and one. A value of one means a perfect correlation a value of zero means no correlation.

Scatter plots with nonlinear curve progressions were standardised before with a best fit estimation (e.g. logarithmic). The type of standardisation function were recognised in the interpretation.

### 3.3.2 Significant difference

A proof of significant difference were used to work out coring sites which differ in their TOC content and performed by running a two sided Welch-test on same parameters (TOC) from two different coring locations. The Welch-test were chosen because of its handling with variabilities in the variance of the different sample-sets.

The principal bases on the test of a assumed null hypothesis  $H_0: \mu_0 = \mu_1$  compared to a alternative hypothesis  $H_a: \mu_0 \neq \mu_1$ , where  $\mu_0$  and  $\mu_1$  are the mean of each sample set (TOC content of a sediment core) (*Precht et al.*, 2005). A difference is evident when the null hypothesis is confuted with a reliability of  $\alpha \leq 0.05$  which is also called p-value. A normal distribution of each sample-set is assumed to run this test.

### 3.3.3 Principal component analysis (PCA)

The PCA is a powerful tool to identify patterns in multivariate data, and expressing the data in such a way as to highlight their similarities and differences (*Smith, 2002; Legendre & Legendre, 2012*). The principle is to reduce redundant informations which occur during a multidimensional regression and concentrate this redundancy in new generated principal components (PC). Thereby, the PC's act as axes of a coordinate system where the transformed environmental variables (species scores) and samples (sample scores) are plotted. Before the transformation of the dataset can be proceed, it is necessary to standardise the dataset. The standardisation is important to enable comparison between

variables expressed in different units and on different scales of measurement (Leyer *et al.*, 2008). The dataset was standardised with a squareroot function for moisture, TOC and TN content and C/N ratio and with a decadic logarithmic function for  $\delta^{13}\text{C}$ . To obtain positive values, the  $\delta^{13}\text{C}$  values were added with a constant of 100.

The transformation of the dataset can be proceed as follows:

- 1.) Estimation of the regression coefficient foreach environmental variable (see Equation 5).
- 2.) Estimation of new sample scores as follows:

$$x_i = \sum_{k=1}^m y_{ki} b_k \quad \text{Eq. 7}$$

Where  $x_i$  are the new sample scores,  $y_{ki}$  are the standardised original samples of a certain coring site and depth and  $b$  the regression coefficient of  $i$  environmental variable.

- 3.) Repetition of step one and two new derived species and sample scores until the scores has stabilised

The derived sample scores can now be plotted in a biplot where the axes represent PC1 and PC2.

The derived species scores represent the absolut value of a vector which is drawn from the center of the biplot. As higher the absolute value as higher the abundancy of the represented environmental variable.

All statistical analyses were performed with the open source software R Studio and the use of the vegan library.

## 4. Results

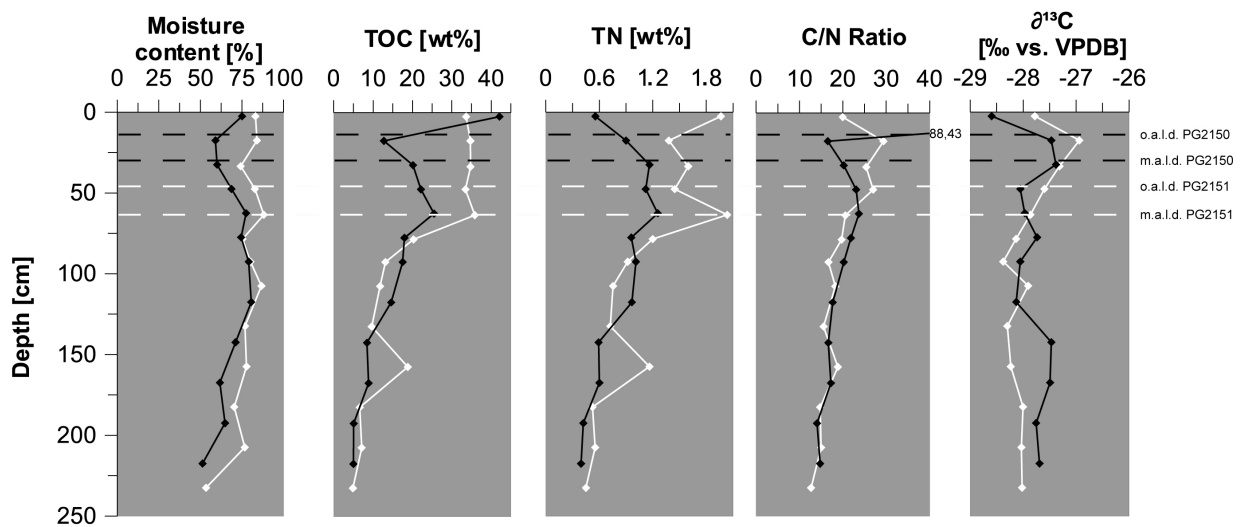
### 4.1 Presentation of moisture content, biogeochemistry and stable carbon isotopes according to ecological units

This chapter comprises the data presentation of moisture content, total organic carbon (TOC) and total nitrogen (TN) content, the atomic ratio between total organic carbon and total nitrogen (C/N) as well as the stable carbon isotope composition on organic carbon ( $\delta^{13}\text{C}$ ). The aim of this chapter is to show trends and differences in the above mentioned parameters and to compare the active layer properties with subjacent permafrost as well as to mention minimum and maximum values. To reach this, the data set was subdivided by core sites and plotted against core depth below surface. The y-axis represents core depth below surface. The x-axis shows the laboratory parameters and the scale was kept constant for each parameter to enable a good comparability between coring locations. Every core plot was marked with the observed active layer depth (o.a.l.d.) and the maximum active layer depth (m.a.l.d.). The o.a.l.d. is the thaw depth at the time when the core was taken but when the maximum seasonal thaw depth was not reached yet. The m.a.l.d. is the long term maximum thaw depth at the end of the thawing season. Pronounced differences in cryostructures and moisture contents occur at the boundary between the long-term seasonal thaw depth and the permafrost table, where water accumulates and refreezes in winter forming distinct cryostructures. It was derived by visual inspection of changes in cryostructure which were observed during core investigation. Total carbon values were not included because TOC is the adequate parameter to depict evidence about organic matter supply and distribution. A complete overview of the dataset in numerical values as well as GPS supported locations of all coring locations are listed in the appendix.

#### 4.1.1 Guillemot unit (PG2150, PG2151)

The Guillemot unit covers approximately 8.64 km<sup>2</sup> (8 %) on Herschel Island. It represents wet polygonal terrain on flat tundra. Ice wedges, polygon centers and cryoturbated soils characterise this unit. Drainage from higher elevations keeps the ground constantly saturated. Erosional features are absent. These conditions may favour organic matter preservation rather than degradation.

Two cores were drilled within the Guillemot unit located at N 69.57957, W 138.95728 (PG2150) and N 69.57952, W 138.95734 (PG2151). One core was located on the polygon rim (PG2150) and the other in the polygon centre (PG2151).



**Figure 4.1** Summary of moisture content, TOC, TN, C/N atomic ratio and  $\delta^{13}\text{C}$  for the Guillemot unit. Black diamonds represent values for core site PG2150, white diamonds for PG2151. Note that the C/N ratio at top active layer of PG2150 (88.43) is out of scale for better visualisation of the rest of data points.

The cryostructures in permafrost in PG2150 alternates between massive and ataxitic from final depth until 83 cm and subsequently change to reticulate and lenticular until the permafrost table. PG2151 shows a similar composition but sediments are more fine grained. The cryostructure is suspended and changes to massive or ataxitic until the permafrost table. Both cores contain ice lenses of varying size (mm to cm) but PG2151 is more ice-rich resulting in a higher moisture content (Fig 4.1). The observed active layer is composed in both cores of fibric to mesic peat, with roots and mosses. Subjacent permafrost in PG2150 comprises dark brown, humic to mesic peat to greyish brown, sandy silt.

In both cores TOC, TN and C/N ratios generally increase, interrupted by a positive peak in TOC and TN of PG2151 at 157.5 cm. Moisture content has no overall trend and shows just minor changes with mean values of around 70 % (PG2150) and 79 % (PG2151). The TOC content of PG2150 shows an decreasing trend from 62.5 cm depth until the o.a.l.d. TOC values in the top active layer differs strongly from all other values with a maximum at 42 %. The core description notes high concentrations of roots and mosses what might be an explanation for this high TOC value. TOC values of PG2151 increase until the permafrost table and show subsequent no trend until the surface. The TN content of PG2150 generally increase until the permafrost table and show an decreasing trend from 1.16 % at the m.a.l.d. to 0.56 % below surface. The TN content of PG2151 increase until permafrost table and show no trend within the active layer. The  $\delta^{13}\text{C}$  composition of PG2150 show minor changes between -28.6 ‰ and -27.4 ‰. PG2151 shows a constant  $\delta^{13}\text{C}$  value

at around -28 ‰ until ca. 78 cm and subsequently increase from -28.4‰ to -26.9 ‰ until surface

#### 4.1.2 Herschel unit (PG2152, PG2154, PG2163)

The Herschel unit represents undisturbed tundra on upland plains and gently rolling terrain and covers approximately 28.18 km<sup>2</sup> (25 %) on the Island. It is characterised by the occasional occurrence of polygonal ground, gentle slopes seldomly exceeding 5 % and a hummocky surface covered by the Cottongrass/Moss vegetation type (*Smith et al.*, 1989). The drainage is imperfect to poor so that the soil is saturated most of the year and cryoturbation occurs.

**Table 4.1** Facies description of permafrost layers in PG2152, PG2154 and PG2163 (Herschel unit)

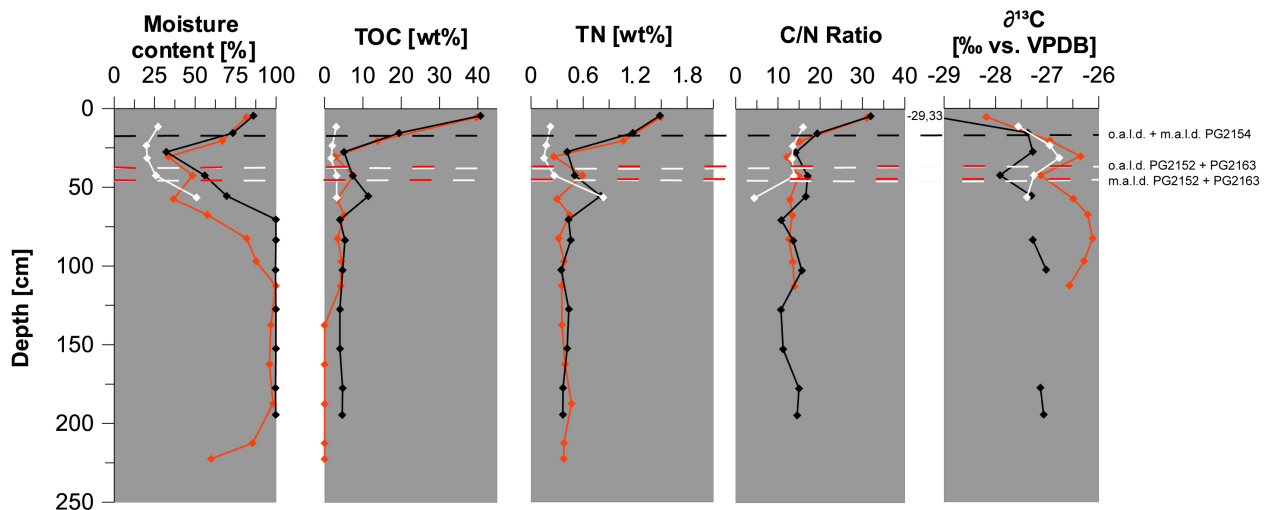
	Depth	Sediment	Organic	Cryostructure	Ice
PG2152	34 – 49 cm	grey to brown sandy silt coarse sand and small gravel	humic to mesic organic clusters	massive	ice poor, reticulate ice lenses
	49 – 59 cm	greyish brown to brown black sandy silt, gravel admixture 2 cm in diameter	black spots of humic organic material	massive	ice poor, subvertical ice lenses
	59 – 63 cm	light grey clayey silt,	humic particles	lenslike reticulate	ice rich
PG2154	18 – 33 cm	dark brown to greyish brown clayey silt	humic organic	porphyric	ice poor
	33 – 59 cm	clayey silt, some gravel up to 5mm	mesic organic, some macro-organic remains	lenslike reticulate	content increase downcore, lenses up to 5 mm thick
	59 – 198 cm	few sediment inclusions	-	-	massive ice wedge
PG2163	33 – 46 cm	light brownish grey clayey silt	well rooted, live roots	fine lenslike reticulate	moderate content
	46 – 59 cm	grey silty clay to brownish grey sandy silt	macro-organic remains	coarse reticulate	moderate content, fine ice lenses
	59 – 95 cm	brownish grey sandy silt	organic rich	ataxitic to suspended	ice rich, verticle bubble trains
	95 – 99 cm	greyish brown sandy peat	mesic organic, some macro-organic remains	porphyric	ice rich, ice lenses. ca. 1 cm length, 2 mm width
	99 – 116 cm	sediment inclusions, greyish brown sandy silt	organic rich	-	ice rich, bubbles
	116 – 192 cm	vertical sediment vein	-	-	ice wedge
	192 – 230 cm	brownish grey silty loam	macro-organic remains	suspended	ice rich

Three cores were drilled within the Herschel unit. PG2152 and PG2154 are located at N 69.57148, W 13802656. PG2163 is located at N 69.57871, W 138.87083. The Permafrost facies characteristics differ from core to core (Tab. 4.1). Massive ice wedges were drilled in PG2154 and PG2163 which caused either limited sediment yield for laboratory analyses or were free of sediment. Detailed permafrost facies description for all three cores are shown in table 4.1. The observed active layer is similarly composed in all three cores of light brown to greyish, clayey to sandy silt inclusions or lenses. Live vegetation, litter and dark brown, fibric to mesic horizons occur at the top active layer. Roots and mosses are present. Some iron oxidation bands occur in PG2152 and PG2154.

The moisture content is lowest in PG2152 with values between 20 and 51 %. PG2154 and PG2163 show similar trends. First, both decrease downcore from ca. 83 % to 33 % and increase again to 100 % due to the presence of an ice wedge which begins at ca. 59 cm (PG2154) and ca. 116 cm (PG2163). PG2152 has low TOC values throughout the core of around 3 %. TOC content in



PG2150 stay constant until 70 cm depth. A subsequent positive peak is evident. In PG2163, sediment contained no TOC until 112.5 cm due to values keep below detection limit. PG2154 and PG2163 show similar trends in TOC in the upper 50 cm with increases until 40 %.



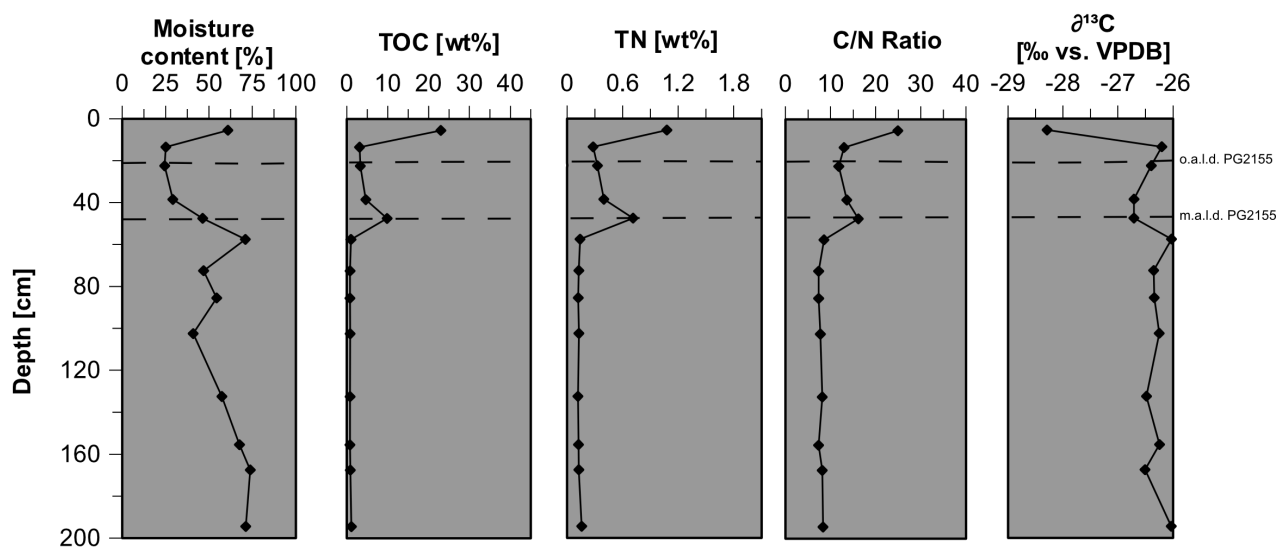
**Figure 4.2** Summary of moisture content, TOC, TN, C/N atomic ratio and  $\delta^{13}\text{C}$  for the Herschel unit. White diamonds represent values for core site PG2152, black diamonds for PG2154 and red diamonds for PG2163. First  $\delta^{13}\text{C}$  value of PG2154 is out scale due to visualisation of the rest of the data points. In PG2154,  $\delta^{13}\text{C}$  values between 63 and 68 cm, 122 and 155 cm and in PG2163, C/N ratio and  $\delta^{13}\text{C}$  values below 135 cm were not obtained due to massive ice wedge occurrence.

The TN content show the same trend as described for TOC. Values range between 1.5 % (maximum for PG2154 and PG2163) and 0.17 % (minimum for PG2152). C/N ratios of PG2152 increase through the active layer from 4 at 56 cm until 16 below surface. No C/N ratios were calculated for PG2163 until 112.5 cm due to not enough sediment sample for TOC measurement. PG2163 keep rather constant in the C/N ratio until 40 cm depth. PG2154 shows no trend and ranges between 10 and 17 until 40 cm depth. Again, C/N ratios for PG2163 and PG2154 show similar trends until surface where C/N ratios increase from 15 (PG2154) and 12 (PG2163) to 31.  $\delta^{13}\text{C}$  values in PG2154 and PG2163 show no major trend until her respective permafrost table with values in the range of -27.9 ‰ and -27 ‰ for PG2154 and -27,1 ‰ and -26,1 ‰ for PG2163. Afterwards, both cores show a positive peak and decrease again until surface to -29.3 ‰ (PG2154) and -28.2‰ (PG2163).  $\delta^{13}\text{C}$  values in PG2152 ranges between -27.6 ‰ and -26.7 ‰.

### 4.1.3 Komakuk unit (PG2155)

The Komakuk unit is the most common eco unit on Herschel Island covering 35.01 km<sup>2</sup> (32 %). It shows strong variation in vegetation and soil properties which is caused by a morphological diversity with a mixture of smooth uplands, transected with minor valleys as well as non-sorted patterned ground. Slopes can be developed in both convex and concave shape leading to moderate to imperfect drainage. The most common soil type is Orthic Turbic Cryosol (*Smith et al.*, 1989).

One core was drilled within the Komakuk unit located at N 69.57467, W 139.00703. Permafrost soils from final depth until 89 cm depth consists of very ice rich grey loam with coarse sediment clusters. The cryostructure is suspended. Sediments until 52 cm depth consist of ice rich grey clayey silt with roots up to 1 mm. The cryostructure changes from suspended to reticulate to suspended again. Overlying permafrost until the o.a.l.d. show grey, silty to sandy loam as well as humic organic with sandy and silty admixtures. The cryostructure is massive with vertical ice lenses and sediment inclusions occur. The observed active layer comprises dark brown mesic peat to brownish grey, clayey to silty loam with some roots. Subangular gravel, varying in size (mm to cm) occasionally occurs.



**Figure 4.3** Summary of moisture content, TOC, TN, C/N atomic ratio and  $\delta^{13}\text{C}$  for PG2155 (Komakuk unit).

The moisture content of PG2155 has no major trend through the core, varying between 74 % and 25 %. TOC, TN and C/N ratio show simultaneous trends through the core with significantly different values between permafrost and the overlying active layer. The TOC, TN and C/N ratio remain rather unchanged until the m.a.l.d. but afterwards increase by trend until the surface. The TOC

content keeps in a narrow range between 0.8 % and 1.1 % from final depth to the m.a.l.d. Afterwards it abruptly increase to a peak at 9.9 % and decrease again to 4.6 %. Another distinct increase is evident at the top active layer sample reaching 23 %. The TN content shows no major changes until the m.a.l.d. with a value of around 0.14 %. At the m.a.l.d. the TN value increase to a positive peak at 0.71 % and subsequent decreases until 0.28 %. A distinct increase is evident at the top active layer reaching 1.08 %. The C/N ratio follows that previous mentioned trend with values range around 8 % until the m.a.l.d., 16 % at the m.a.l.d. and 25 % in the top active layer. The  $\delta^{13}\text{C}$  value keep rather unchanged until below of the top active layer sample and increases than from -26.2 ‰-28.3 ‰.

#### 4.1.4 Orca unit (PG2156, PG2159)

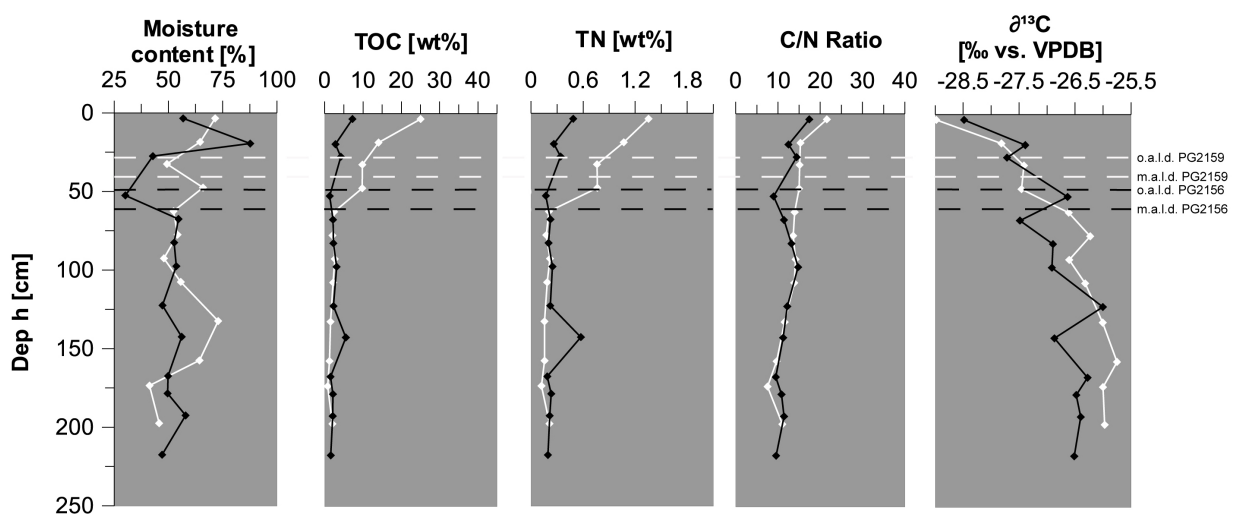
The Orca unit covers 1,25 km<sup>2</sup> (1 %) on Herschel Island. It is characterised by very gently sloped alluvial fans or floodplains which arouses prior sandy silt to clayey silt. Surface drainage occurs in form of little stream channels and active deposition takes place. In these channels more coarse material may occur. The active layer reaches depths up to 60 cm in a regosolic to gleyosolic static cryosol. The vegetation varies between willows in better drained areas to sedges in area where standing water occurs.

**Table 4.2** Facies description of permafrost layers in PG2156, and PG2159.

	Depth	Sediment	Organic matter	Cryostructure	Ice
PG2156	49 – 60 cm	gray clay	rooted	massive	ice poor
	60 – 67 cm	grey clayey silt	occasional roots	lenslike reticulate to irregular reticulate	increasing ice content, Fine ice lenses
	67 – 72 cm	grey clayey silt	occasional roots	suspended	ice rich
	72 – 84 cm	grey clayey silt	occasional roots	lenslike reticulate, parallel to wavy	ice lenses < 1 cm
	84 – 84,5 cm	-	layer of organic material	-	-
	84,5 – 119 cm	grey clayey silt	organic macrofossils	microlenticular to lenticular	ice lenses
	119 – 142 cm	grey clayey silt	some macro-organic inclusions	reticulate to suspended	ice rich
	142 – 144 cm	organic layer, brownish black	woody macrofossils	massive	ice rich
	144 – 178 cm	grey clayey silt	some macro-organic inclusions	suspended to reticulate	ice rich
	178 – 227 cm	grey clayey loam to silty sand Increasing in grain size	macro-organic remains	alternation between reticulate & suspended	ice rich, vertical elongated bubbles > 1 mm
PG2159	28 – 43 cm	dark greyish brown sandy silt	humic, macro-organic Remains	massive	moderate ice content
	43 – 59 cm	grey sandy silt	organic rich, macro-organic remains	porphyric	ice rich
	59 – 103 cm	grey sandy silt	less organic	lenslike reticulate	very ice rich
	128 – 142 cm	grey sandy silt	less organic	suspended	very ice rich
	142 – 169 cm	grey silty clay coarsening down-core	organic macrofossils	suspended with reticulate patches	ice rich, vertical elongated bubbles > 1 mm
	169 – 173 cm	dark grey silty fine sand	organic rich, macro-organic remains	micro-lenticular	ice rich
	173 – 176 cm	greenish grey fine sand	organic rich, macro-organic remains	porphyric	ice rich
	176 – 187 cm	grey silty to fine sand	organic rich	micro-lenticular	moderate ice content
	187 – 195 cm	grey silty loam	organic rich	lenslike to fine reticulate	moderate ice content
	195 – 200 cm	sandy silt to fine sand	organic rich	lenslike to fine reticulate	moderate ice content

Two cores were drilled within the Orca unit located at N 69.57082, W 138.89462 (PG2156) and N 69.57340, W 138.99677. The active layer contains dark brown, mesic to fibric organics and brownish grey, silty clay. In addition, PG2156 is well rooted through the whole active layer. The subjacent permafrost changes frequently in material and cryostructure and is described in detail in table 4.2.

The moisture content in PG2156 remains rather constant until m.a.l.d. at around 50 %. Within the active layer it varies between 30 % and 88 % PG2159 show no trend through the whole core and varies in range of 72 % and 41 %. PG2156 show little changes in TOC content with moderate to low values between 7 % to 1 %. No distinct changes between the active layer and the subjacent permafrost are evident. A distinct trend in TOC values occur in PG2159 between the permafrost and above of the m.a.l.d.. At first, the TN value remain rather constant at around 2 % until 55 cm depth. Afterwards, it continuous increases throughout the m.a.l.d. until the surface and reaches a value of 25 %. The TN values in PG2156 and PG2159 exhibit the same trend as described for TOC. The values for PG2156 range between 0.57 % and 0.17 %. PG2159 remain rather unchanged at around 0.19 % until 55cm depth and increases then until the surface to 1.35 %. The C/N ratios in both cores show a slight overall increase until the surface from ca. 9.5 (PG2156) and ca. 11 (PG2159) to ca. 22 (PG2156) and ca. 17 (PG2159). No differences are visible between the permafrost and overlying active layer. A distinct overall decrease until the surface of  $\delta^{13}\text{C}$  values is evident for both cores.  $\delta^{13}\text{C}$  in PG2156 overall decreases with interruptions from -26 ‰ to -28.5 ‰. PG2159 overall decreases with little interruptions from -26 ‰ to -29 ‰. No distinct differences are visible in both cores between active layer and subjacent permafrost.



**Figure 4.4** Summary of moisture content, TOC, TN, C/N atomic ratio and  $\delta^{13}\text{C}$  for the Orca unit. Black diamonds represent values for core site PG2156, white diamonds for PG2159.

#### 4.1.5 Plover + Jaeger unit (PG2157, PG2162)

These formerly separately characterised units (*Smith et al.*, 1989) cover 24.14km<sup>2</sup> (22 %) of Herschel Island.

It can be regarded as a transition zone between smooth uplands (see Komakuk unit) and strong erosive slopes and gullies (see 4.1.6., Thrasher unit). The morphology varies between few non sorted nets to more common, moderate slopes and ridges where mass movement processes occurs. The ground is moderate to well drained. Soil erosion leading to a more exposed soil than at the Komakuk unit. The soil type varies between cryoturbated soils where patterned ground occurs to regosolic static cryosol at gullied sites.

Two cores were drilled within these units located at N 69.57398, W 138.88455 (PG2157) and N 69.58010, W 138.90816 (PG2162). The active layer in PG2157 comprises dark brown to brownish grey silty loam with sandy inclusions, organic rich patches and occasional living roots. The active layer in PG2162 shows a more diverse characterisation which is described in table 4.3. The permafrost were not sampled because of gravel prohibited coring.

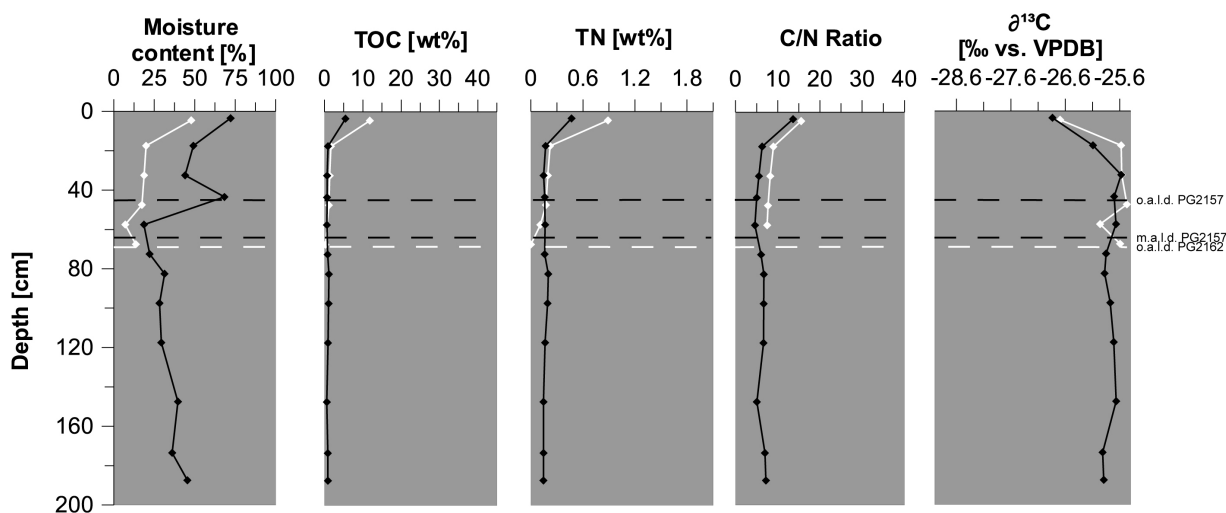
**Table 4.3** Facies description of active layer in PG2162 (Jaeger unit)

	Depth	Sediment	Organic matter
	0 – 1 cm	-	live vegetation
	1 – 7 cm	dark brown, silty sand	mesic to humic organic, well rooted
PG2162	7 – 26 cm	grey to brownish grey, sandy loam	peat lenses/ organic lenses, Well-rooted
	26 – 41 cm	grey sandy loam, material sorting into lenses and patches of fine (clayey) material and coarse (sandy) material	rooted, organic rich lenses
	41 – 61 cm	grey sandy loam, abundant gravel up to 3 cm	still live roots
	61 – 70 cm	grey silty sand, loam lenses of 1 cm thickness	macro-organic remains

The permafrost facies in PG2157 exhibit more homogenous sediments through the core with grey, silty loam. No roots occur anymore but occasional carbonate shell fragments (e.g. at 58 cm depth). The cryostructure is alternating between reticulate (irregular and lenslike), ataxitic and suspended. The ice content gradually decreases against the m.a.l.d..

The moisture content in the active layer of PG2162 increases against the surface from 13 % to 48 %. PG2157 moisture content decreases from 45 % at final depth to 19 % at the m.a.l.d. Subsequently, it increases to 68 % at the o.a.l.d. and remain unconstant until the top active layer where it reaches the maximum of 72 %. The TOC does not change much until below top active layer with a value of around 2 % but increases then to 5 % (PG2157) and 12 % (PG2162). The TN

content has the same signature where to remain in general below 0.2 % and only increase at 15 cm to 0.47 % (PG2157) and 0.89 % (PG2162). The C/N ratio remain rather unchanged for both cores at roughly 7 and increases as well at the same depth to around 14 %. In the  $\delta^{13}\text{C}$  signature, PG2157 shows no major changes until the o.a.l.d.. Both cores exhibit a little decrease at 30 cm depth (PG2157) and 15 cm depth until the surface from ca. -26.7 ‰ to -25.6 ‰.



**Figure 4.5** Summary of moisture content, TOC, TN, C/N atomic ratio and  $\delta^{13}\text{C}$  for the Plover and Jaeger unit. Black diamonds represent values for core site PG2157, white diamonds for PG2162. Note that for PG2162 gravel prohibited drilling, only a pit was dug. The last C/N ratio were not determined due to no TN content at that sample point.

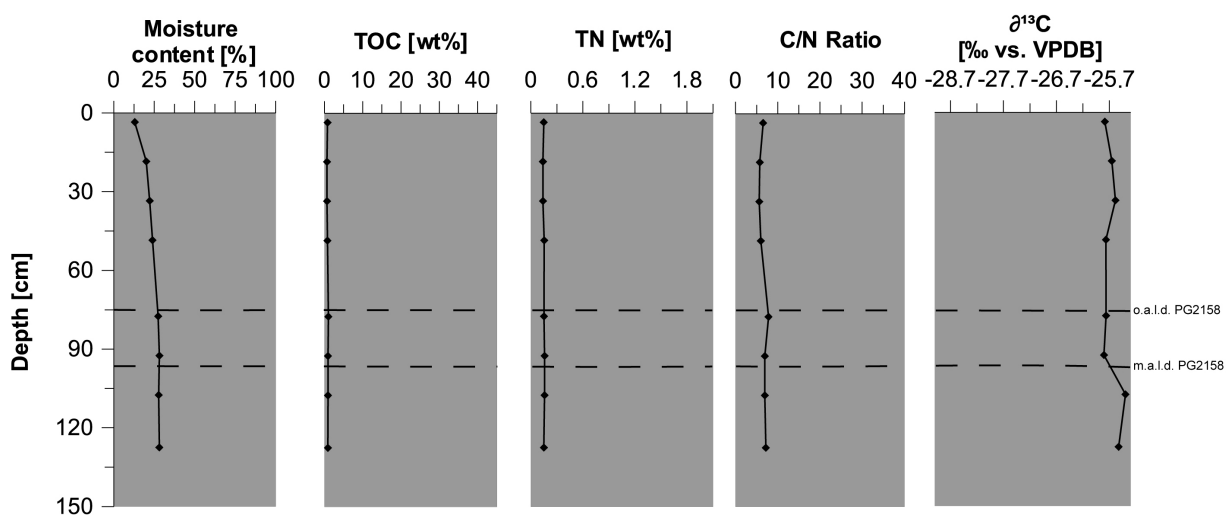
#### 4.1.6 Thrasher Unit (PG2158)

The Thrasher unit covers 12.59 km<sup>2</sup> (11 %) on Herschel Island and is characterised by a strongly sloping terrain with steep gullies, mass movement and erosion. Coastal bluffs and retrogressive thaw slumps add to this unit. The soil is generally well-drained and solifluction as well as gelifluction occur depending on the slope gradient. Mass movement and erosion usually prohibit the development of a humic horizon so that the vegetation cover is generally low and the active layer can reach up to 100 cm depth. The major soil type is regosolic static cryosol.

One core was drilled within the Thrasher unit located at N 69.57600, W 138.89360. The permafrost comprises greyish silty clay with occasional gravel. Tiny black spots (< 1 mm) of humic organic occur. The cryostructure is massive to porphyric. The overlying active layer consist of highly consolidated, grey silty clay with occasional gravel; subangular and up to 2 cm in size. Carbonate shell fragments occur.

All parameter have almost lineally trend against the surface and show no changes between the

permafrost and the overlying active layer. The moisture content continuous decrease from ca. 28 % to 13 %. The TOC content remains below 1 % throughout the core. The same applies to the TN content which remains below 0.16 %. The C/N ratio moves in a narrow range between 8 and 6.  $\delta^{13}\text{C}$  values show minor changes which not exceed  $25,5\text{‰} \pm 0.4\text{‰}$ .



**Figure 4.6** Summary of moisture content, TOC, TN, C/N atomic ratio and  $\delta^{13}\text{C}$  for PG2158 (Thrasher unit).

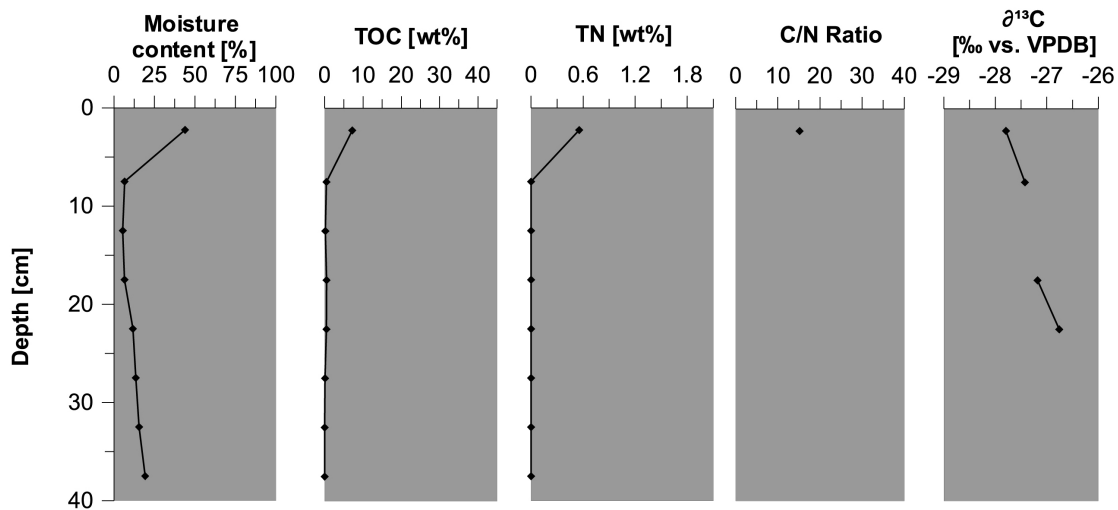
#### 4.1.7 Avadlek unit (J01)

The Avadlek unit comprises all coastlines, lagoons and spits around Herschel Island and covers an area of 1.08 km<sup>2</sup> (1%). It differs strongly from all other units in vegetation, soil condition and active layer depth. Generally it reflects unconsolidated material consisting of medium to coarse grained material (preferential sand and gravel) which is due to marine erosion and deposition. The setting of the eco unit is caused by its location at or slightly above the sea level where the sea water temperature raises the active layer depth. Low moisture content is caused by coarse material where high porosity causes rapid drainage and a low preservation potential of soil organic matter.

A pit was dug within this unit located at N 69.56835, W 138.92037. Information about the active layer are limited because water filled the pit beginning at 40cm. Generally, it comprises organic bearing, medium to coarse grained sand with occasionally gravel bands and living roots. Pebbles of more than 15 cm in diameter occur at 21 cm depth. The material is getting coarser with increasing depth.

The moisture content is low with a mean of 15 %. TOC values above device-specific detection limit were only obtained between 15 cm and 25 cm and as well between 10 cm and the surface and

remains below 1 %. The TN content were obtained just for the first sample point with 0.55 %. Consequently, the C/N ratios and  $\delta^{13}\text{C}$  values are missing.



**Figure 4.7** Summary of moisture content, TOC, TN, C/N atomic ratio and  $\delta^{13}\text{C}$  for J01 (Avadlek unit). Note that all samples were taken from the active layer. C/N ratios below 5 cm could not be determined due to TN values below device-specific detection limit.  $\delta^{13}\text{C}$  values below 25 cm and between 10 and 15 cm could not be determined due to TOC values below device-specific detection limit.



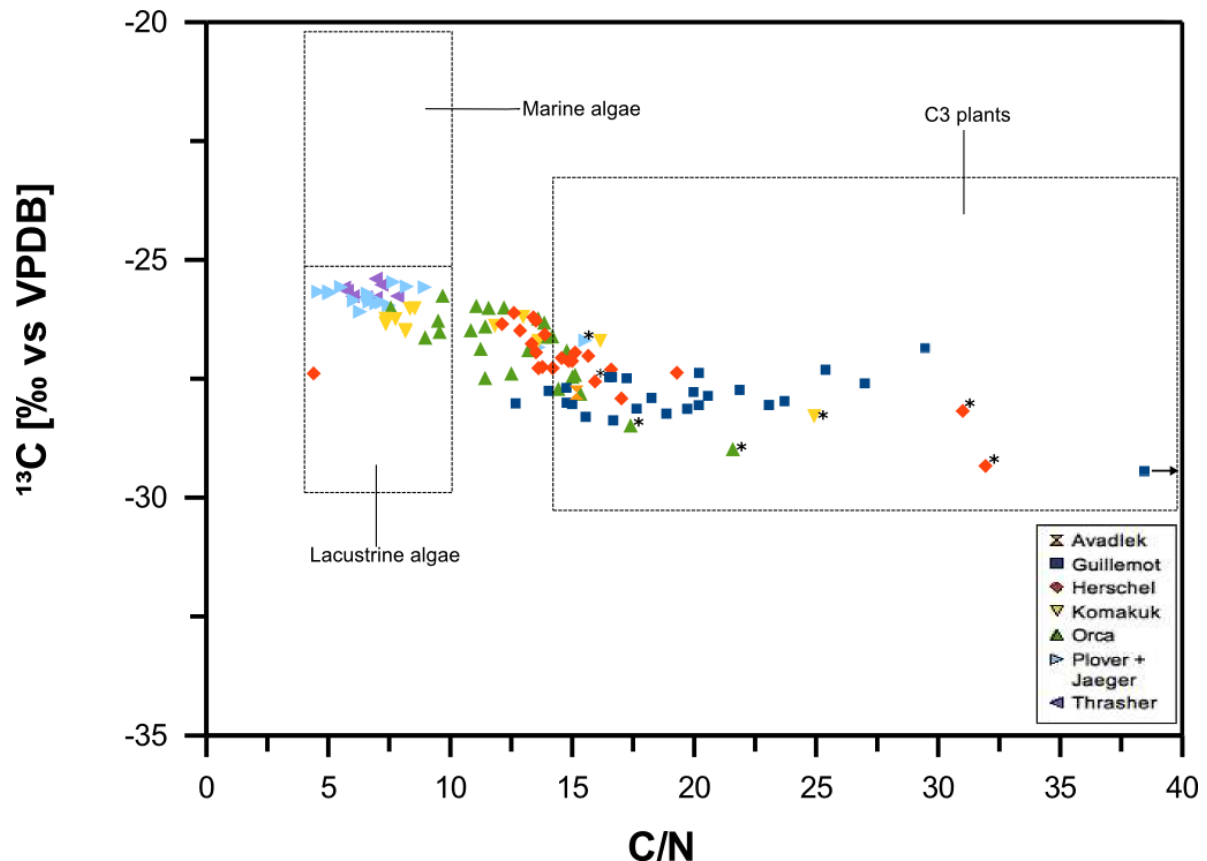
## 5. Discussion

This chapter is divided into three parts. The first part links the soil organic matter (SOM) with its biotic source. Possible differences in the biotic signal between the active layer and subjacent permafrost as well as between the eco units will be discussed in the matter of preservation versus modification of the original signal. The second part examines the eco units in the light of preservation or degradation status of organic matter under consideration of its surface and subsurface qualities. Standard deviations of TOC, best fit regressions and statistical significance analyses will be used to classify the eco units in representative groups of SOM quality. Finally, the third part links the biogeochemical parameters and stable carbon isotope signatures with possible modern environmental parameters using principal component analysis (PCA).

### 5.1 Origin of soil organic matter in surficial permafrost

The comparison of  $\delta^{13}\text{C}$  values and the C/N ratio can be used to distinguish between C3 plants, C4 plants, marine algae and lacustrine algae and is hence a helpful tool to possibly identify the biotic signature of organic matter in soils of Herschel Island. However, this original signature can change over time. Selective degradation of organic matter during early diagenesis has the potential to modify C/N ratios in sediments (Meyers, 2001). Figure 5.1 shows the distribution of all samples grouped according to eco units. Similar to Fritz (2008), the distribution of the main sample composition shows a generally mixed signal between C3 plants and algae. This supports the view of formerly marine nearshore sediments that have been pushed as an endmoraine during the Late Glacial Maximum, which is today Herschel. (Bouchard, 1974; Rampton, 1982; Fritz, 2008). With the onset of a warmer climate at the beginning of the Holocene, an establishment of a C3 vegetation has a cumulative influence on SOM expressed in a broadening of the C/N ratio distribution (Fig. 5.1) Except from PG2158, all uppermost active layer samples (0-10 cm, Fig. 5.1) exhibit C/N ratios substantially higher than subjacent samples which support this view. Accompanied, the plot shows a decrease of C/N ratios linked with an increasing trend of disturbance of the depositional environment. This trend is caused by preferential loss of low molecular-weight carbon compounds (primarily carbon and starch) through aerobic decay (Kuhry *et al.*, 1996). Instances for this phenomena are cores from the Herschel, Orca and Komakuk unit which show at first a decrease of C/N ratios with depth (from the surface until approximately 20 cm depth) initiating from the C3 plant box and moving leftward (Fig. 5.1). Afterwards, C/N ratios range between 9 and 15 which overlaps with values observed for algae species (Meyer, 1994). Permafrost samples from the

Komakuk unit are considered to be of glacial age and older (M. Fritz, 2014, personal communication) which is emphasized by the fact that all permafrost samples plot within the algae box. For the Herschel, Komakuk, and Orca unit it remains yet unclear where the original signal of the C/N ratio begins and where the modification ends.



**Figure 5.1** Elemental (atomic C/N ratio) and isotopic ( $\delta^{13}\text{C}$  value) identifiers of bulk organic matter produced by marine algae, lacustrine algae and C3 plants. C4 plants box is excluded due to no relevance in the Arctic. Note that due to better clarity, sample PG2150\_0-5 cm (C/N ratio: 88.4,  $\delta^{13}\text{C}$ : -28.6) is outside the plot marked with an arrow. represent with blue box at right edge. Asterixes mark uppermost active layer samples. (adapted from Meyers, 1997, modified)

Samples from the Guillemot unit plot almost completely within the C3 plant box. The assumption that these samples are considered to be of Holocene age (M. Fritz, 2014, personal communication) is supported by post-glacial C3 vegetation establishment that represents the original source in this unit. Samples from the Plover, Jaeger and Thrasher unit show C/N ratios in a very narrow range between approximately 9 and 5 plot in the algae box. Only the uppermost active layer samples (0 - 10 cm) from the Plover and Jaeger unit (PG2157 and PG2162) are higher with values of 14 and 16 respectively and located in C3 box. These distinct box allocation of the samples may represent

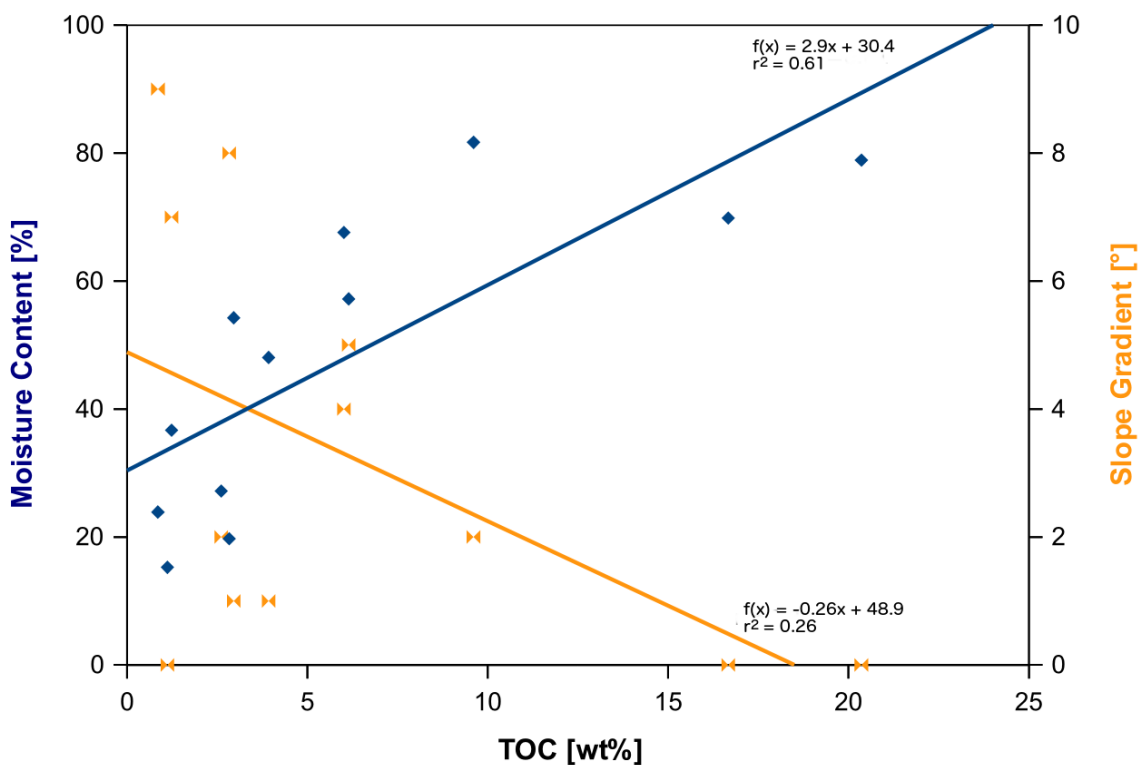
original signatures of modern C3 vegetation and old marine algae in the Plover and Jaeger unit. The higher C/N ratios in uppermost active layer samples might be caused by recent net primary production. Subjacent samples might represent old refractory material that survived redistribution processes and accompanied mineralisation (e.g. slumping, active layer detachments) in this location. This might be the same explanation for the Thrasher unit where ongoing surface erosion or incomplete slope stabilization (*Lantuit et al.*, 2012) are responsible for the absence of net primary production and organic matter preservation, and hence no increased C/N ratio at the top active layer. The  $\delta^{13}\text{C}$  values plot in a narrow range between -25‰ and -29‰ which are typical values for the Beaufort Sea shelf region (*Naidu et al.*, 1999). A slight increase of  $\delta^{13}\text{C}$  values is linked to a transition from C3 plants to algae. More negative  $\delta^{13}\text{C}$  values in uppermost active layer samples of Komakuk, Orca and Herschel units might be explained by input of litter of *Salix* and *Carex* into the ground which contributes to  $\delta^{13}\text{C}$  values between -28‰ and -30‰ (*Loader et al.* 2006, *Skrzypek et al.*, 2008). Higher percentages of moss in PG2151 (Guillemot unit) might contribute to slightly higher  $\delta^{13}\text{C}$  values (*Hornibrook et al.*, 2009). The general shift to higher  $\delta^{13}\text{C}$  values C3 vegetation to the algae box the is caused by an increase of decomposition (*Hornibrook et al.*, 2009) and go along with C/N ratio decrease.  $\delta^{13}\text{C}$  values of algae species can vary depending on the  $\delta^{13}\text{C}$  signature of dissolved  $\text{CO}_2$  in the water.  $^{13}\text{C}$  concentrations in  $\text{CO}_2$  are affected by surface water temperatures in oceans and lakes, increasing during cooler times and decreasing during warmer periods (Meyers, 1997). This could be the case for samples that plot in the lacustrine algae field but are considered to be as marine algae, because organic matter produced by marine algae living in cold polar waters has  $\delta^{13}\text{C}$  values as low as -28‰, which is in the range of lacustrine algae (*Rau et al.*, 1989). SOM in permafrost samples from the Herschel and Komakuk unit and most samples from Thrasher, Plover and Jaeger unit reflect detectors probably originate from past glacial times.

## 5.2 Preservation and degradation of soil organic matter in surficial permafrost

The results chapter indicated that Herschel Island exhibit a heterogeneous SOM and stable carbon isotope signature even between coring sites within the same eco units. This limits the value of the eco unit classification established by *Smith* (1989) about the soil organic matter distribution. A development of a renewed classification with respect to gradients of TOC and TN decomposition might be helpful. On the other hand, the lack of good marker beds (*Fritz*, 2008) as well as few radio carbon dates makes it difficult to execute an adequate comparison between the same parameters across the different coring sites and therefore across eco units. However, the investigation of surface and subsurface conditions and their correlation with TOC and TN might be helpful to estimate the preservation and degradation status in the active layer and surficial permafrost.

### 5.2.1 Surface versus subsurface conditions

Besides the moisture content, biogeochemistry and stable carbon isotope signatures, the slope angle, slope orientation, and percentage of bare ground (see Tab. 2.1) are other important measurable factors to characterise ground disturbance and bioproductivity. Figure 5.2 shows the mean TOC content for every eco unit as a function of associated slope angle and mean moisture content. The mean TOC content is positively correlated with the moisture content ( $r^2 = 0.61$ ,  $n = 12$ ) and negatively correlated with the slope angle ( $r^2 = 0.26$ ,  $n = 12$ ) which generally represents drainage conditions. The higher coefficient of determination between moisture content and TOC content represents a better reproduction of the heterogenic conditions downcore. However, the slope angle might have a major influence on surface erosion, drainage conditions and percentage of bare ground when it exceeds a certain threshold.



**Figure 5.2** Correlation of moisture content and slope gradient with the mean TOC content of each core.  $r^2$  represents the coefficient of determination for each linear regression.

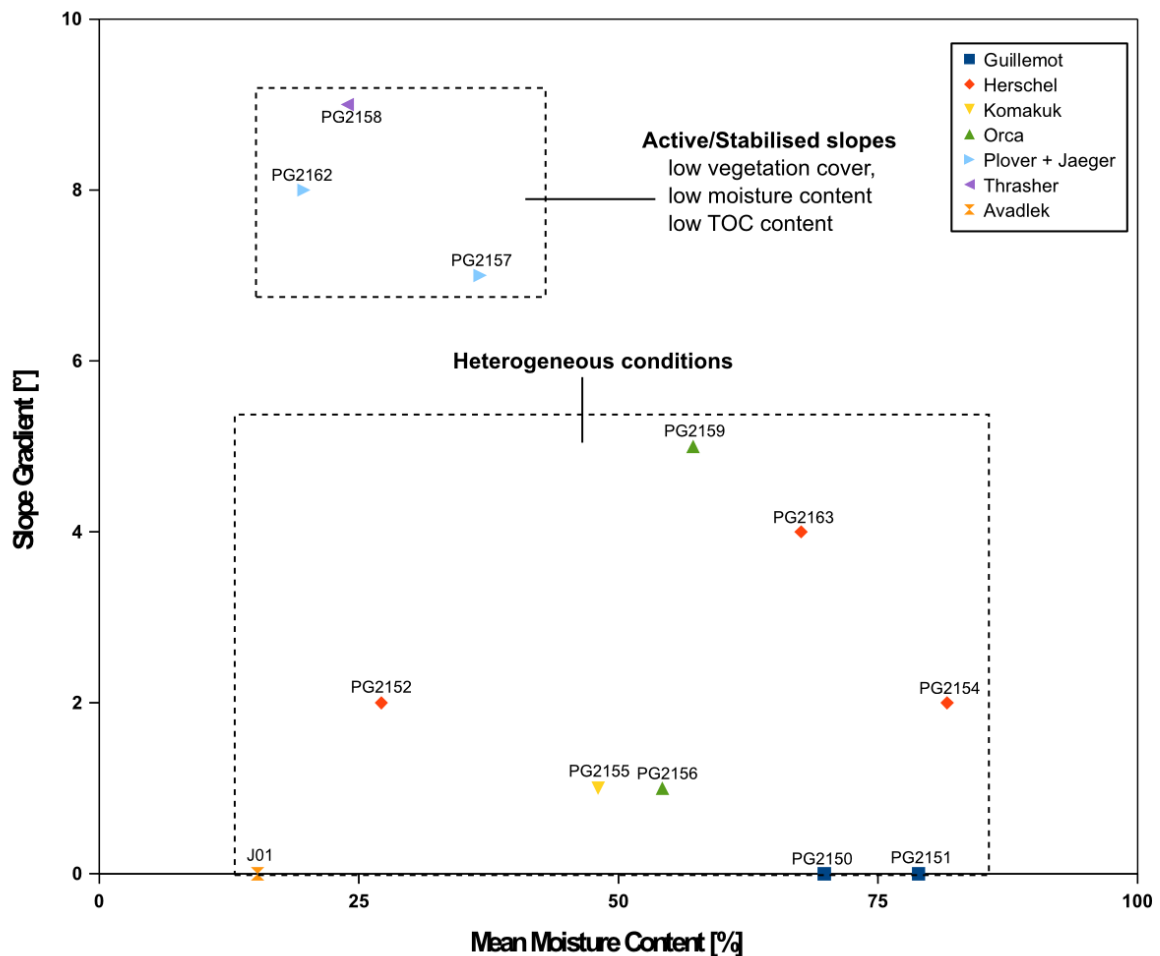
### 5.2.2 Mass wasting and stabilised slopes

*McRoberts and Morgenstern* (1974) showed that active layer detachments in similar environments occurs at slope angles between three and nine degrees. From this it follows that slow mass wasting phenomena begin already at low slope angles as it occurs on Herschel Island. Mass wasting phenomena such as solifluction and creep induce ground disturbance and can lead to improved aeration and hence strong mineralisation of fresh litter. This in turn limit the metabolism of fresh litter into SOM. *Wolfe* (2001) and *Lantuit et al.* (2012) observed that stabilised slopes on Herschel Island (where thaw slides and retrogressive slumps were active) are capable to reestablish a vegetation cover. Ground disturbance and reestablishment of a slope might be a good explanation for the Thrasher, Plover and Jaeger unit. PG2157 (Plover) and PG2162 (Jaeger) show a slight increase in TOC and TN values in the uppermost active layer samples while the subjacent ground is depleted in these contents due to former disturbance by glacial ice thrust and subsequent mass wasting phenomena. Low mean TOC contents (Tab. 2.1) support that assumption of a consistently depleted ground. The stabilisation of a slope depends on the quantity of massive ground ice below the shear plane (*Lantuit et al.* 2012) and the fraction of fines which possess high ductility. PG2158 (Thrasher) possibly represents the onset of a stabilisation where a low vegetation cover produce no considerable SOM yet.

The result is a advanced classification of the cores into two groups with respect to slope angle and moisture content as show in Figure 5.3. The upper box, represents cores with distinct characteristics of mass wasting phenomena or stabilisation of a slope with reestablished vegetation cover (PG2157, PG2162, PG2158). Low mean moistue contents (37% for PG2157, 24% for PG2158 and 20% for PG2162) and medium to high percentages of bare ground (20% for PG2157, 80% for PG2158, and 5% for PG2162, see also Tab. 2.1) are the consequence and aeffect biomass production. The orientation of the slope affect additionally the distribution of a vegetation cover (*Price*, 1973). The lower box in Figure 5.3 represents a widespread range of surface and subsurface conditions with slope gradients between 0° and 5° and moisture contents between 20% and 80%. Coring sites which plot within this box are less affected by surface erosion or have been stabilised since longer time. Other qualities such as grain size, and cryostructure have a stronger control than mass wasting on moisture content and soil organic matter (e.g. *Schnitzer et al.*, 1978). These coring sites show higher TOC and TN values not only in the uppermost active layer samples so that they should be considered separately.

**Table 5.1** Overview of different observed and calculated qualities of slope, moisture and TOC content. Standard deviations were obtained from TOC sample set of each core. Type of regression and Coefficient of determination were obtained by TOC vs. Depth correlation and represent the individual best fit for each coring site. No regression was realised for PG2152 due to no representative results.

Eco unit (classified)	Coring site	Slope gradient [°]	Mean moisture content [%]	Mean TOC content [wt%]	Standard deviation	Type of Regression	Coefficient of determination (r <sup>2</sup> )	Number of samples (n)
Avadlek	J01	0	15,26	1,12	2,47	polynomial	0.76	8
Guillemot	PG2150	0	69,83	16,67	10,39	logarithmic	0.79	12
Guillemot	PG2151	0	78,91	20,36	12,41	logarithmic	0.84	13
Herschel	PG2152	2	27,17	2,61	0,69	-	-	5
Herschel	PG2154	2	81,67	9,6	10,77	exponential	0.76	12
Herschel	PG2163	4	67,59	6,01	11,85	exponential	0.79	9
Komakuk	PG2155	1	48,06	3,92	2,7	polynomial	0.68	13
Orca	PG2156	1	54,25	2,95	1,73	exponential	0.45	13
Orca	PG2159	5	57,2	6,14	7,36	polynomial	0.83	12
Plover	PG2157	7	36,69	1,23	1,34	polynomial	0.5	12
Jaeger	PG2162	8	19,72	2,83	4,44	polynomial	0.9	6
Thrasher	PG2158	9	23,89	0,85	0,13	linear	0.53	8



**Figure 5.3** Classification of the coring sites with respect to slope gradient and mean moisture content in active/stabilised (after Lantuit *et al.*, 2012) and heterogenous.

### 5.2.3 Peatland development

PG2150 and PG2151 from the Guillemot unit possess a significantly higher TOC content than the other units (Tab. 5.1 and Tab. 5.2) which refers to a different development of the subsurface. Consequently, the Guillemot unit be considered separately.

Organic matter supply under similar conditions from the Usa Basin, Russia (*Hugelius et al.*, 2011), from Truelove lowland, Devon Island, Canada (*Somr et al.* 1991) and different locations on Herschel Island (*Kokelj et al.* 2002) show a similar distribution of TOC with depth. Here, the rate of biomass production is greater than the rate of decomposition (*Kuhry et al.*, 1996). Cryoturbation is present in silty, loamy soils and has been shown to reduce the decomposition rate of SOM as it moves SOM into deeper soil layers (*Washburn*, 1980, *Kaiser et al.*, 2007; *Xu et al.*, 2009). In PG2150 and PG2151 the active layer can be subdivided into an acrotelm (aerobic conditions) and a catotelm (anaerobic conditions; Fig. 5.4). In the acrotelm the organic carbon and nitrogen content has undergone mineraliation by bacterial activity leading to a CO<sub>2</sub> and NH<sub>4</sub> production (*Schlesinger*, 1997; *Bundy*, 1998). Most of the mineralised carbon will be released to the atmosphere or reabsorbed by plants (*Schlesinger*, 1997). The residual carbon goes to the catotelm where additional loss occurs by e.g. methanogenesis and sulphate reduction. NH<sub>4</sub> is partly undergone nitrification what leads to a nitrogen enrichment in the catotelm (*Kuhry et al.* 1996, Fig. 4.1). Anaerobic decay of residual organic matter process considerably slower and organic matter accumulation is potential.

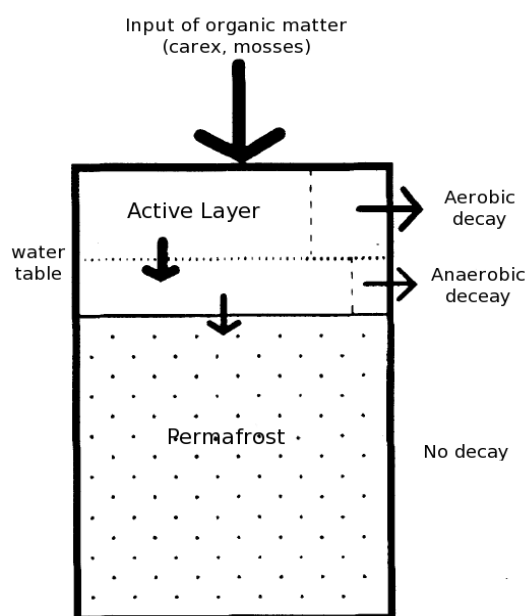
**Table 5.2** Statistical significance of T-test in R for TOC contents between the Guillemot unit (PG2150, PG2151) and the other coring sites. Significance is evident when  $P \leq 0.05$ . No significance between PG2150 and PG2154 is marked with italic numbers.

Coring sites	PG2152	PG2154	PG2155	PG2156	PG2157	PG2158	PG2159	PG2162	PG2163
PG2150	0.01	<i>0.12</i>	0.002	0.0008	0.0003	0.0003	0.0009	0.003	0.05
PG2151	<0.0001	0.02	0.0004	0.0002	0.0001	0.0001	0.001	<0.0001	0.01

Active layer samples from PG2150 and PG2151 represent above described processes by enrichment of TOC and TN values until the maximum active layer depth (Fig 4.1). Higher values in the active layer of PG2151 refers to its location in a polygon centre. A constant TOC values until the m.a.l.d. is caused by quiet deposit conditions where an acrotelm is poorly developed. In contrast, PG2150 is located on a polygon rim where the proximity to an ice wedge and slightly coarser sediments (silt, sand) lead to more intense oxygen percolation resulting in a deeper developed acrotelm. Subjacent permafrost until final core depth at PG2150 and PG2151 has lower TOC and TN contents than the overlying active layer but still considerable. This suggests that high bioproductivity and OM

preservation occurred already during former sedimentation which supports a Holocene age for PG2150 and PG2151 (Fritz et al., unpublished data). Logarithmic regressions for both cores support a low gradient of degradation downcore as it observed in peatland environments (Kuhry et al. 1996; Tab. 5.2).

The Guillemot shows ombrogenous characteristics as observed at bog milieus (Vitt et al. 1994). It is associated with lowland ice-wedge polygons (Hugelius et al., 2010). Acidic soils,  $\delta^{18}\text{O}$  values of around -17‰, which represents water from Holocene precipitation (Fritz et al., unpublished data), and the high surface cover with sphagnum moss (20%) at both coring sites supports this assumption.



**Figure 5.4** Schematic diagram of decay of organic matter in peatlands underlain by permafrost. (adapted from Vardy et al., 1999, modified)

#### 5.2.4 Eco units with heterogeneous subsurface conditions

Coring sites from the Herschel, Komakuk and Orca unit have a significantly lower organic matter contents than the Guillemot unit (Tab. 5.1 and 5.2). Moreover, they show distinct differences in the shape of their depth plot for TOC and TN content. PG2155 (Komakuk), PG2154 and PG2163 (both Herschel) exhibit sharp gradients of TOC and TN decrease with depth while the PG2150 and PG2151 (Guillemot unit) exhibit a smooth TOC and TN gradient with depth. This suggests different rates of sedimentation (Zimov et al., 2009) and hence different ages with depth. PG2155, PG2154 and PG2163 are located on elevated terrain and upland plateaus where low sedimentation rates are occur. Consequently, the depositional age increases faster with depth than in depressions where



more intense sediment input occurs.

PG2154 and PG2163 show less significant differences in their TOC contents compared to Guillemot coring sites (Tab. 5.2, italic value). This can be explained by strong input of SOM in the active layer at undisturbed upland plateaus. *Kokelj et al. (2002)* observed on a coring site near located to PG2163 a similar active layer depth and similar TOC contents within the active layer depth. A complete vegetation cover of prior *Eriophorum* tussocks and high moisture contents in the active layer support high biomass production and less decay.

The subjacent permafrost in PG2154 and PG2163 is depleted and homogenous until final depth. *Zimov et al. (2009)* showed that in cold permafrost regions where no or little sedimentation occurs, the TOC content strongly accumulates with wetter conditions in the top active layer but not necessarily penetrates to deeper horizons what. This could be a good explanation for an abrupt TOC decrease in PG2154, PG2163. Occurring gravel admixtures through the active layer which lead to a higher aeration and less SOM preservation might be an additional explanation. PG2152 exhibit low organic carbon production and low TOC and TN content even in the top active layer although it shows the same soil conditions, no differences in elevation, type of vegetation cover and percentage of bare ground were observed. The reason for this difference in TOC and TN content however remains unclear. Due to its contrast in TOC and TN values between PG2154, PG2163 and PG2152, the Herschel unit is considered to be heterogeneous in its SOM properties. The Orca unit draw also a heterogeneous picture in its SOM properties. PG2159 show distinct preservation of TOC and TN in the active layer. This is supported by a standard deviation of 7.36 which is more close to standard deviations from the Herschel and Guillemot unit (Tab. 5.1). A smoother gradient in the decrease of TOC and TN content suggest more active deposition in comparison to the Herschel and Komakuk unit. This agrees with its proximity to a slope where runoff is present. Waterlogging lead to limited decomposition and supports a good SOM preservation throughout the active layer at PG2159. PG2156 shows similar vegetation and soil characteristics but no distinct storage of TOC and TN in the active layer. Its location on a lobe on a floodplain might be indicative of high deposition rates and good aeration leading to a lower bio mass production. An intermediate increase of TOC and TN in PG2156 refers rather to incorporation of woody macrofossil which survived decomposition.

### 5.3 Possible explanation of biogeochemistry and stable carbon isotope characteristics with the help of environmental statistical tools

Figure 5.5 shows an unconstrained ordination of the dataset derived by principal component analysis (PCA) (see chapter 3.3 for detailed explanation). Principal components one and two explain 72.6 % and 14.5 % of the variation in the data set. The sample scores and variable scores are shown in the appendix.

The C/N ratio, TOC and TN content are positively correlated with the PC1 axis and negatively correlated with the PC2 axis. They are associated with active layer sample scores from the peatland class and top active layer sample scores from units characterised as heterogeneous (4th quadrant, Fig 5.5). They reflect bio mass production and a good SOM preservation. Active layer sample scores from unit classified as peatland correlate positively with TOC and TN content and correspond with thick surface organic deposits and a shallow permafrost table. Both top active layer sample scores from peatland sites exhibit the highest PC1 scores and most negative PC2 scores. This suggests waterlogging and strong input of live vegetation which exceed microbial activity leading here to a SOM accumulation. However, it's location at the margin of the diagram suggest to consider these samples as less representative (*Leyer et al., 2008*). Uppermost active layer samples from heterogeneous sites show highest correlation with the C/N ratio (Fig. 5.5.). Subjacent active layer samples are located more close to the center of the plot (zero) with very low correlation to the C/N ratio. This signify fast decomposition of SOM within the active layer at heterogeneous characterised units.

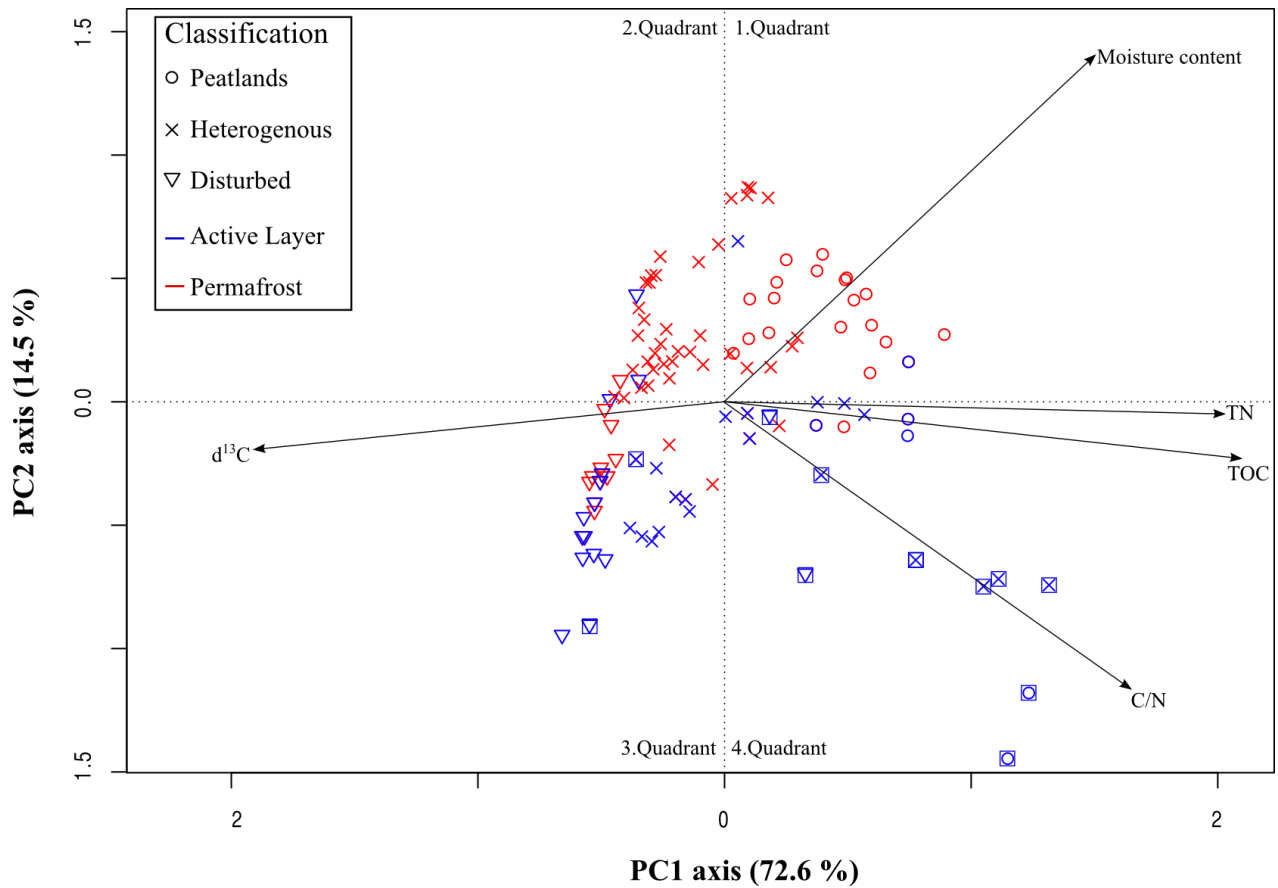
Moisture content shows both a positive correlation with the PC1 axis and a positive correlation with the PC2 axis and is associated with permafrost horizons from the peatland class (Fig. 5.5, red circles). No correlation between moisture content and C/N ratio suggest that high ice contents in deeper soils explain moisture content better than thaw or precipitation induced water in the active layer. Moreover, the permafrost samples are driven by moderate to organic rich and ice rich soils with changing cryostructures. This may reflect changing phases of warmer and colder conditions with a lowering and rising permafrost table as it occurs during the early and middle Holocene (*Fritz et al., 2012b*).

In contrast, the  $\delta^{13}\text{C}$  variable is negatively correlated with both axes. Her negative correlation with the TOC and TN content underline to be an indicator of degradation. A slightly negative correlation with the moisture content reflect rapid drainage and agree with high disturbance. Consequently, OM depleted samples from disturbed units are characterised by a elevated  $\delta^{13}\text{C}$  composition. A cluster of permafrost sample scores from heterogeneous units are located in the second quadrant reflecting high ice contents and low organic matter contents. They show less variability than

peatland permafrost samples and might be indicative for more stable conditions during formation. On the other hand, its negative correlation with the C/N ratio might indicate that former intense decomposition took place and homogenised this soil horizon. Permafrost samples from heterogeneous units exhibit the highest PC2 scores and correspond to observed ice wedges in PG2154 and PG2163.

A gradient in soil moisture is proposed along the PC2 axis as indicated by positively correlated permafrost sample scores (red symbols) and negatively correlated active layer sample scores (blue symbols, samples considered until the m.a.l.d.). Along the first PC axis a SOM storage gradient is evident. This emphasises the role of young peatlands in depressions as being rich in organic carbon and a good accumulator of litter. The second PC axis is driven by moisture quality and activity. It is indicated by a clear gradient between disturbed and heterogeneous sites on negative hand side along the first axis and between the active layer and permafrost within the peatland sites on the positive side along the first axis. This shows that surface drainage has a strong influence on the ability to preserve SOM in the active layer on Herschel Island.

The PCA diagramm shows that morphologically more heterogeneous sites (Herschel, Komakuk, Orca) contain higher variability in its potential to store SOM than more homogeneous peatlands and disturbed units. Moreover, it shows that the moisture content has a strong effect on soil conditions and hence to favour or prohibit SOM preservation on Herschel Island.



**Figure 5.5** PCA ordination diagram showing TOC, TN, C/N ratio and  $\delta^{13}\text{C}$  as response variables (solid black arrow) as well as active layer (blue) and permafrost (red) samples of observed eco units. Eco units are classified in peatlands (Guillemot unit, marked with circles), heterogeneous (Herschel, Komakuk and Orca units, marked with crosses) and disturbed (Jaeger, Plover and Thrasher units, marked with triangles). Uppermost active layer samples are marked with square boxes. PC axis 1 and 2 explain 72.6 % and 14.5 % of the variance in the data set, respectively.

## 6. Conclusions & Outlook

SOM in the active layer and surficial permafrost on Herschel Island in the western Canadian Arctic is governed by partly distinct and partly by heterogeneous surface and subsurface conditions. The following suggested classification of the existing ecological units shows that Herschel Island reflects a heterogeneous landscape affected by differences in slope, vegetation cover and vegetation type, soil type and moisture content. These parameters in turn affect the preservation and degradation of SOM. The following specific conclusions can be drawn from this study:

### *Peatlands (Guillemot)*

- Consistently high TOC and TN contents throughout the active layer indicate strong biomass production and good preservation of soil organic matter in waterlogged, anaerobic soil horizons
- Smooth gradients in TOC and TN suggest additionally higher sedimentation rates supplied from surrounded elevated terrain.

### Heterogeneous units (Herschel, Komakuk, Orca)

- Strong input of SOM in the active layer is evident.
- Decrease in C/N ratios and an increase in  $\delta^{13}\text{C}$  indicate increased decomposition with depth leading to reduced SOM content in the subjacent permafrost at all coring sites compared to peatlands.
- Uncertainties remain because of contrasting observations at coring sites with similar morphology, vegetation and soil conditions

### *Disturbed units (Jaeger, Plover, Thrasher)*

- Mass wasting, bare ground and good drainage occur in these units leading to well-aerated soils and reduces or even prohibits biomass production and hence the input of SOM
- SOM is suggested to be remobilised during disturbance and subsequently degraded
- Consequently, all disturbed coring sites show lowest TOC and TN contents in the active layer and subjacent permafrost
- Stabilised slopes show evidence of reestablishment of a vegetation cover leading to an initiation of SOM input

The TOC and TN content, the C/N ratio as well as  $\delta^{13}\text{C}$  composition emphasize their roles to be good indicators for the biotic origin as well as for the degradation and preservation status of SOM. Suggestions about paleoenvironmental conditions and changes which have contributed to the observed SOM content are still difficult. Radiocarbon age determinations could help to better link the different SOM contents with past stages of the Pleistocene and Holocene. Near surface air temperatures play an additional role for energy fluxes into the active layer which in turn, have major impacts on the thaw depth and hence on the remobilisation of SOM. Unfortunately, continuous recordings of ground temperature are missing and should be recognised in future investigations. Summer precipitation contributes to the surficial ground water content and the growth of vegetation and hence to the quantity of biomass production. In combination with soil nutrients, changes in the precipitation rates may influence the height and percentage of the vegetation cover and should be also considered. All these above mentioned variables can be added to the existing PCA to improve its significance. Finally, the quantification of biomarkers such as phospholipid fatty acids (*Pautler et al.*, 2009) can give information about which biochemical compounds preferentially survive microbial activity and hence represent residual SOM in the active layer and surficial permafrost on Herschel Island.

## 7. References

- Bouchard, M.*, (1974). Surficial Geology of Herschel Island, Yukon Territory. M.Sc. thesis, University of Montreal, 70p.
- Bundy, L. G.*, (1998). Soil and applied Nitrogen. University of Wisconsin Extension
- Burn, C. R., Zhang, Y.*, (2009). Permafrost and climate change at Herschel Island (Qikiqtaruq), Yukon Territory, Canada. *Journal of Geophysical Research*, Vol.114.
- Craig, H.*, (1953). The geochemistry of the stable carbon isotopes. *Geochimica et Cosmochimica Acta*, Vol. 3, pp. 53 - 92
- Crum., H., Planisek, S.*, (1992). A focus on peatlands and peat mosses (Great Lakes Environment). Univ. of Michigan Pr., 320p.
- Dansgaard, W.*, (1953). Comparative measurements of standards for carbon isotopes. *Geochimica et Cosmochimica Acta* 3, pp. 253 - 256
- Dyke, A. S., Andrews, J. T., Clark, P. U., England, J. H., Miller, G. H., Shawe, J., Veillette, J. J.*, (2002). The Laurentide and Innuitian ice sheets during the Last Glacial Maximum. *Quaternary Science Review*, Vol. 21, pp. 9 - 31
- French, H. M.*, (2007). *The Periglacial Environment*. 3rd edition, John Wiley & Sons, Ltd, 458p.
- Fritz, M.*, (2008). Late Quaternary paleoenvironmental records from a glacially and permafrost affected island in the Canadian Arctic (Herschel Island, Yukon Coastal Plain). Diplomarbeit zur Erlangung des akademischen Grades Diplom-Geograph, 135 p
- Fritz, M., Wetterich, S., Meyer, H., Schirrmeister, L., Lantuit, H., Pollard, W. H.*, (2011) Origin and Characteristics of Massive Ground Ice on Herschel Island (Western Canadian Arctic) as revealed by Stable Water Isotope and Hydrochemical Signatures. *Permafrost and Permafrost and Periglacial Processes*, Vol. 22, pp. 26 - 38
- Fritz, M., Wetterich, S., Schirrmeister, L., Meyer, H., Lantuit, H., Preusser, F., Pollard, W. H.*, (2012). Eastern Beringia and beyond: Late Wisconsinan and Holocene landscape dynamics along the Yukon Coastal Plain, Canada. *Palaeogeography, Palaeoclimatology, Palaeoecology*, pp. 28 - 45
- Fritz, M., Herzschuh, U., Wetterich, S., H., Lantuit, de Pascale, G. P., F., Pollard, W. H., Schirrmeister, L.*, (2012). Late Glacial and Holocene sedimentation, vegetation and climate history from easternmost Beringia (northern Yukon Territory, Canada). *Quaternary Research*, Vol. 78, pp. 549 - 580
- Gorham, E.*, (1991). Northern Peatlands: Role in the Carbon Cycle and Probable Responses to Climatic Warming. *Ecological Applications*, Vol. 1, pp. 182 - 195
- Hayes, J. M.*, (1993). Factors controlling  $^{13}\text{C}$  contents of sedimentary organic compounds: Principles and evidence. *Marine Geology*, Vol. 113, pp. 111 - 125

- Hornibrook, E. R. C., Longstaffe, F. J., Fyfe, W. S., Bloom, Y.* (2000). Carbon-isotope ratios and carbon, nitrogen and sulfur abundances in flora and soil organic matter from a temperate-zone bog and marsh. *Geochemical Journal*, Vol. 34, pp. 237 - 245
- Hugelius, G., Kuhry, P.* (2009). Landscape partitioning and environmental gradient analyses of soil organic carbon in a permafrost environment. *Global biogeochemical cycles*, Vol 23,
- Hugelius, G., Kuhry, P., Tarnocai, C., Virtanen, T.* (2010). Soil organic carbon pools in a periglacial landscape: a case study from the central canadian arctic. *Permafrost and periglacial processes*, Vol. 21, pp. 16 - 29
- Hugelius, G., Routh, J., Kuhry, P., Crill, P.* (2010). Chemical characteristics and lability of soil organic matter in permafrost terrain, european russian arctic, Department of physical geography and quaternary geology
- IPCC* (2007). *Climate Change 2007: The Physical Science Basis*. Contribution of Working Group I to the Fourth Assessment Report of the Intergovernmental Panel on Climate Change. Cambridge University Press. Cambridge.
- Karte, J.* (1979). Räumliche Abgrenzung und regionale Differenzierung des Periglazials. *Bochumer Geographische Arbeiten* 35. Göttingen.
- Kuhry, P., Vitt, D. H.* (1996). Fossil carbon/nitrogen ratios as a measure of peat decomposition. *Ecology*, Vol. 77, pp. 271 - 275
- Kuhry, P., Dorrepaal, E., Hugelius, G., Schuur, E. A. G., Tarnocai, C.* (2010). Potential remobilization of below ground permafrost carbon under future global warming. *Permafrost and Periglacial Processes*, Vol. 21, pp. 208 - 214
- Lantuit, H., Pollard, W. H.* (2005). Temporal stereophotogrammetric analysis of retrogressive thaw slumps on Herschel Island, Yukon Territory. *Natural Hazards and Earth System Sciences*, Vol. 5, pp. 413 - 423
- Lantuit, H., Pollard, W. H.* (2008). Fifty years of coastal erosion and retrogressive thaw slump activity on Herschel Island, southern Beaufort Sea, Yukon Territory, Canada. *Geomorphology*, Vol. 95, pp. 84 - 102
- Lantuit, H., Pollard, W. H., Couture, N., Fritz, M., Schirmer, L., Meyer, H., Hubberten, H.-W.* (2012). Modern and Late Holocene Retrogressive Thaw Slump Activity on the Yukon Coastal Plain and Herschel Island, Yukon Territory, Canada. *Permafrost and Perigl. Process.*, Vol. 23, pp. 39 - 51
- Lenz, J.* (2010). Late Quaternary landscape dynamics in the Western Canadian Arctic derived from lake sediments on Herschel Island (Southern Beaufort Sea). Diplomarbeit zur Erlangung des akademischen Grades Diplom-Geographin, 83p.
- Leyer, I., Wesche, K.* (2008). *Multivariate Statistik in der Ökologie*. Springer Verlag Berlin-Heidelberg, 217p.
- Loader, N. J., Rundgren, M.* (2006). The role of inter-specific, micro-habitat and climatic factors on the carbon isotope ( $\delta^{13}\text{C}$ ) variability of a modern leaf assemblage from northern Scandinavia: implications for climate reconstruction. *Boreas*, Vol. 35, pp. 188 - 201



- Legendre, P., Legendre, L.*, (2012). Numerical Ecology. Developments in Environmental Modelling, Vol. 24, Third English Edition, 969 p
- Lunardini V. J.*, (1991). Heat transfer with freezing and thawing. Elsevier Science Publishers B.V., 437p.
- Mackay, J. R.*, (1972). Offshore permafrost and ground ice, southern Beaufort Sea, Canada. Canadian Journal of Earth Sciences, Vol. 9, pp. 1550 - 1561
- Mackay, J. R.*, (1972). The World of Underground Ice. Annals of the Association of American Geographers, Vol. 62, pp. 1 - 22
- Meyers, P. A.*, (1994). Preservation of elemental and isotopic source identification of sedimentary organic matter. Chemical Geology, Vol. 114, pp. 289 - 302
- Meyers, P. A.*, (1997). Organic geochemical proxies of paleoceanographic, paleolimnologic and paleoclimatic processes. Org. Gechem., Vol. 27, No. 5/6, pp. 213 - 250
- Meyers, P. A., Teranes, J. L.*, (2001). Sediment Organic Matter. Tracking Environmental Change Using Lake Sediments. Volume 5: Physical and Geochemical Methods. Kluwer Academic Publishers, Dordrecht.
- Naidu, A. S., Cooper, L. W., Finney, B. P., MacDonald, R. W., Alexander, C., Semiletov, I. P.*, (1999). Organic carbon isotope ratios ( $\delta^{13}\text{C}$ ) of Arctic Amerasian Continental shelf sediments. Int J Earth Sciences, Vol. 89, pp. 522 - 532
- Nakai, N.*, (1972). Carbon isotopic variation and the paleoclimate of sediments from Lake Biwa. Proceedings of the Japanese Academy, Vol. 48, pp. 516 - 521
- Pautler, B. G., Simpson, A. J., McNally, D. J., Lamoureux, S. F., Simpson, M. J.*, (2010). Arctic Permafrost Active Layer Detachments stimulate Microbial Activity and Degradation of Soil Organic Matter. Environ. Sci. Technol., Vol. 44, pp. 4076 - 4082
- Precht, M., Kraft, R., Bachmaier, M.*, (2005). Angewandte Statistik. Oldenbourg Verlag, 7. Auflage, 301 p
- Price, L. W.*, (1974). Rates of mass wasting in the Ruby Range, Yukon Territory. Permafrost: North American contribution, Vol. 2, pp. 235 - 246
- Rampton, V. N.*, (1982). Quaternary Geology Of The Yukon Coastal Plain. Geological Survey of Canada, Bulletin 317, 49p.
- Rau, G. H., Takahashi, T., DesMarais, D. J.*, (1989). Latitudinal variations in plankton  $\delta^{13}\text{C}$ : Implications for  $\text{CO}_2$  and productivity in past oceans. Nature, Vol. 341, pp. 541- 518
- Schlesinger, W. H.*, (1997). Biogeochemistry. 2nd Edition, Academic Press Limited, 588 p
- Schnitzer, M., Khan, S. U.*, (1978). Soil organic matter. Elsevier Science Publisher B. V., 319 p

- Schuur, E. A. G., Bockheim, J., Canadell, J., Euskirchen, E., Field, C.B., Goryachkin, S.V., Hagemann, S., Kuhry, P., Lafleur, P., Lee, H., Mazhitova, G., Nelson, F. E., Rinke, A., Romanovsky, V., Shiklomanov, N., Tarnocai, C, Venevsky S, Vogel JG, Zimov S. A., (2008).* Vulnerability of permafrost carbon to climate change: implications for the global carbon cycle. *Bioscience*, Vol. 58, pp. 701 - 714
- Skrzypek, G., Paul, D., Wojtun, B, (2008).* Stable isotope composition of plants and peat from Arctic mire and geothermal area in Iceland. *Polish Polar Research*, Vol. 29, pp. 365 - 376
- Smith, C. A. S., Kennedy, C. E., Hargrave, A. E., McKenna, K. M., (1989).* Soil and vegetation of Herschel Island, Yukon Territory. Yukon Soil Survey Report No. 1, Land Resource Research Centre, Agriculture Canada: Ottawa.
- Somr. C. H., King, R. H., (1991).* Origin of Polygonal Peat Plateaus under Conditions of Continuous Permafrost, Truelove Lowland, Devon Island, N.W.T. Phd Thesis, Univerity of Western Ontario
- Tarnocai, C., Canadell, J. G., Schuur, E. A. G., Kuhry, P., Mazhitova, G., Zimov, S., (2009).* Soil organic carbon pools in the northern circumpolar permafrost region. *Global Biogeochemical Cycles*, Vol. 23
- UNEP, (2012).* Policy implications of warming permafrost.
- Van Everdingen, R., (1998).* Glosary of permafrost and related ground-ice terms. Nationional snow and ice data Center/World Data Center for glaciology, Boulder, C.O.
- Vardy, S. R., Warner, B. G., Turunen, J., Aravena, R., (2000).* Carbon accumulation in Permafrost peatlands in the Northwest Territories and Nunavut, Canada. *The Holocene*, Vol. 10, pp. 273 - 280
- Vitt, D. H., Halsey, L. A., Zoltai, S. C., (1994).* The bog landforms of continental western Canada in relation to climate and permafrost patterns. *Arctic and Alpine Research*, Vol. 26, pp. 1 - 13
- Volken, E., Brönnimann, S., (2011)* The thermal zones of the Earth according to the duration of hot, moderate and cold periods and to the impact of heat on the organic world. Translated version of original paper by *W. Köppen (1884)*, *Meteorologische Zeitschrift*, Vol. 20, pp. 351 - 360
- Wolfe, S. A., Kotler, E., Dallimore, S. R., (2001).* Surficial Characteristics and the Distribution of Thaw Landforms (1970 to 1999), Shingle Point to Kay Point, Yukon Territory. Geological Survey of Canada, Terrain Science Division, Open File 4115
- Zhang, T., Barry, R. G., Knowles, K., Heginbottom, J. A., Brown, J., (1999).* Statistics and Characteristics of permafrost and ground-ice distribution in the northern hemisphere. *Polar Geography*, Vol. 23, No. 2, pp. 132 - 154
- Zimov, S. A., Schuur, E. A. G., Chapin III, F. S., (2006).* Permafrost and the Global Carbon Budget. *Science*, Vol. 312, pp. 1612 - 1613

- 
- Zimov, N. S., Zimov, S. A., Zimova, A. E., Zimova, G. M., Chuprynin, V. I., Chapin III, F. S.,*  
(2009). Carbon storage in permafrost and soils of the mammoth tundra-steppe biome: Role  
in the global carbon budget. *Geophysical Research Letters*, Vol. 36, L02502

## 8. Appendix

This chapter provide the numerical dataset from sedimental and statistical analyses and is divided as follows:

### Appendix 1

list of GPS supported coring locations

### Appendix 2

Overview about the dataset derived from field observations and laboratory analysis

### Appendix 3

List of explainable variables scores and sample scores derived by principal component analysis (PCA)

#### Appendix 1: GPS supported coring locations

Eco unit	Core name	GPS name	NAD83 UTM zone 7N		Geographical WGS84	
			X	Y	Longitude	Latitude
Avadlek	J01	Av1	581008,98	7719116,28	-138,9204	69,5684
Guillemot	PG2150, PG2151	Gu1	579965,57	7720439,7	-138,9460	69,5805
Herschel	PG2163	He21	582963,67	7720285,04	-138,8692	69,5782
Herschel	PG2152, PG2154	He4	576761,13	7719320,38	-139,0292	69,5714
Komakuk	PG2155	Ko2	577741,61	7719538,23	-139,0038	69,5731
Orca	PG2156	Or1	581920,44	7719619,55	-138,8966	69,5726
Orca	PG2159	Or2	578071,59	7719586,63	-138,9967	69,5732
Plover	PG2157	Pl1	582382,18	7719791,1	-138,8846	69,5740
Jaeger	PG2162	Ja1	581440,1	7720440,96	-138,9952	69,5735
Thrasher	PG2158	Th1	580303,12	7720012,57	-138,9377	69,5766

**Appendix 2:** Sample list with results from field observations and elemental analysis. 128 samples were taken during field work.

-\*: value were under the device-specific detection limit

-\*\*: no calculation possible due to no available data

Name	Eco Unit	Start depth (cm)	End depth (cm)	Thickness (cm)	Average depth		Sample surface area		Wet sample weight (g)	Dry Sample weight (g)	Moisture content (%)	N g (%)	C g (%)	TOC (%)	C/N atomic ratio	$\delta^{13}C$
					(cm)	Permafrost	(cm <sup>2</sup> )	Volume (cm <sup>3</sup> )								
J01_0-4,5	Av	0	4,5	4,5	2,25	n	56,25	253,13			43,94	0,55	8,22	7,20	15,17	-27,79
J01_5-10	Av	5	10	5	7,5	n	56,25	281,25			6,51	*	1,60	0,48	-**	-27,42
J01_10-15	Av	10	15	5	12,5	n	56,25	281,25			5,36	*	1,45	0,18	-**	-**
J01_15-20	Av	15	20	5	17,5	n	56,25	281,25			6,49	*	1,79	0,49	-**	-27,18
J01_20-25	Av	20	25	5	22,5	n	56,25	281,25			11,61	*	1,71	0,48	-**	-26,76
J01_25-30	Av	25	30	5	27,5	n	56,25	281,25			13,43	*	1,50	0,10	-**	-**
J01_30-35	Av	30	35	5	32,5	n	56,25	281,25			15,48	*	1,36	*	-**	-**
J01_35-40	Av	35	40	5	37,5	n	56,25	281,25			19,24	*	1,22	*	-**	-**
PG2150_0-5	Gu	0	5	5	2,5	n	56,25	281,25	50,02	12,47	75,07	0,56	42,15	42,08	88,43	-28,59
PG2150_15-20	Gu	15	20	5	17,5	y	23,93	119,63	217,2	88,83	59,10	0,90	13,78	12,74	16,52	-27,47
PG2150_30-35	Gu	30	35	5	32,5	y	23,93	119,63	222,69	88,93	60,07	1,16	20,14	20,14	20,19	-27,38
PG2150_45-50	Gu	45	50	5	47,5	y	23,93	119,63	211,09	66,08	68,70	1,12	22,15	22,15	23,07	-28,05
PG2150_60-65	Gu	60	65	5	62,5	y	23,93	119,63	188,9	42,64	77,43	1,26	25,50	25,50	23,7	-27,97
PG2150_75-80	Gu	75	80	5	77,5	y	23,93	119,63	180,3	46,1	74,43	0,96	17,96	17,96	21,86	-27,74
PG2150_90-95	Gu	90	95	5	92,5	y	23,93	119,63	210,95	44,19	79,05	1,01	18,22	17,48	20,19	-28,05
PG2150_115-120	Gu	115	120	5	117,5	y	23,93	119,63	207,59	40,38	80,55	0,97	16,53	14,59	17,63	-28,13
PG2150_140-145	Gu	140	145	5	142,5	y	23,93	119,63	209,1	60,33	71,15	0,59	9,62	8,43	16,64	-27,47
PG2150_165-170	Gu	165	170	5	167,5	y	23,93	119,63	237,81	91,02	61,73	0,60	9,77	8,87	17,23	-27,49
PG2150_190-195	Gu	190	195	5	192,5	y	23,93	119,63	243,69	85,69	64,84	0,42	6,19	5,06	14,03	-27,76
PG2150_215-220	Gu	215	220	5	217,5	y	23,93	119,63	268,49	130,64	51,34	0,40	5,97	5,01	14,76	-27,69
PG2151_0-5	Gu	0	5	5	2,5	n	56,25	281,25	266,18	45,02	83,09	1,96	33,61	33,61	19,97	-27,78
PG2151_15-20	Gu	15	20	5	17,5	n	56,25	281,25	281,89	45,1	84,00	1,38	34,73	34,73	29,38	-26,94
PG2151_31-36	Gu	31	36	5	33,5	y	23,93	119,63	189,06	48,68	74,25	1,60	34,76	34,76	25,38	-27,31
PG2151_45-50	Gu	45	50	5	47,5	y	23,93	119,63	185,64	31,99	82,77	1,45	33,46	33,46	26,99	-27,60
PG2151_61-66	Gu	61	66	5	63,5	y	23,93	119,63	196,03	23,26	88,13	2,03	35,83	35,83	20,56	-27,86
PG2151_76-81	Gu	76	81	5	78,5	y	23,93	119,63	209,53	51,68	75,33	1,20	20,26	20,26	19,71	-28,13
PG2151_90-95	Gu	90	95	5	92,5	y	23,93	119,63	218,18	43,36	80,13	0,92	14,03	13,12	16,68	-28,38
PG2151_105-110	Gu	105	110	5	107,5	y	23,93	119,63	185,27	24,59	86,73	0,75	12,67	11,79	18,25	-27,90
PG2151_130-135	Gu	130	135	5	132,5	y	23,93	119,63	243	56,24	76,86	0,72	10,40	9,64	15,55	-28,30
PG2151_155-160	Gu	155	160	5	157,5	y	23,93	119,63	199,55	44,43	77,73	1,16	18,81	18,81	18,86	-28,23
PG2151_180-185	Gu	180	185	5	182,5	y	23,93	119,63	221,35	65,65	70,34	0,52	7,08	6,62	14,77	-28,00
PG2151_205-210	Gu	205	210	5	207,5	y	23,93	119,63	219,29	51,24	76,63	0,55	7,69	7,11	14,99	-28,03
PG2151_230-235	Gu	230	235	5	232,5	y	23,93	119,63	281,82	131,3	53,41	0,45	5,81	4,88	12,68	-28,02
PG2152_9-14	He	9	14	5	11,5	n	56,25	281,25	247,74	180,52	27,13	0,22	3,37	3,04	15,94	-27,56
PG2152_21-26	He	21	26	5	23,5	n	56,25	281,25	442,35	354,08	19,95	0,17	2,29	2,01	13,51	-26,95
PG2152_29-34	He	29	34	5	31,5	n	56,25	281,25	615,55	490,15	20,37	0,15	1,88	1,72	13,34	-26,77
PG2152_40-45	He	40	45	5	42,5	y	23,93	119,63	344,56	255,81	25,76	0,27	3,80	3,14	13,77	-27,26
PG2152_54-59	He	54	59	5	56,5	y	23,93	119,63	253,25	124,25	50,94	0,83	15,14	3,14	4,4	-27,39
PG2154_2-7	He	2	7	5	4,5	n	56,25	281,25	82,53	11,52	86,04	1,49	40,68	40,68	31,94	-29,33
PG2154_13-18	He	13	18	5	15,5	n	56,25	281,25	255,39	68,06	73,35	1,17	22,27	19,41	19,28	-27,38
PG2154_25-30	He	25	30	5	27,5	y	23,93	119,63	288,63	195,46	32,28	0,42	5,96	5,07	14,2	-27,28
PG2154_40-45	He	40	45	5	42,5	y	23,93	119,63	252,99	111,28	56,01	0,50	7,72	7,33	17,02	-27,91
PG2154_53-58	He	53	58	5	55,5	y	23,93	119,63	221,08	67,28	69,57	0,80	12,17	11,40	16,6	-27,31
PG2154_68-73	He	68	73	5	70,5	y	23,93	119,63	191,89	0,1	99,95	0,43	6,41	4,00	10,8	not enough Material
PG2154_81-86	He	81	86	5	83,5	y	23,93	119,63	203,21	0,1	99,95	0,46	6,28	5,33	13,62	-27,28
PG2154_100-105	He	100	105	5	102,5	y	23,93	119,63	183,83	0,52	99,72	0,35	5,30	4,67	15,66	-27,02
PG2154_125-130	He	125	130	5	127,5	y	23,93	119,63	177,67	0,1	99,94	0,44	6,78	4,00	10,72	not enough Material
PG2154_150-155	He	150	155	5	152,5	y	23,93	119,63	184,78	0,1	99,95	0,42	5,23	4,00	11,23	not enough Material

PG2154_175-180	He	175	180	5	177,5	y	23,93	119,63	141,27	0,43	99,70	0,37	5,41	4,73	14,99	-27,13
PG2154_192-197	He	192	197	5	194,5	y	23,93	119,63	185,52	0,35	99,81	0,37	5,14	4,59	14,57	-27,07
PG2163_3-8	He	3	8	5	5,5	n	56,25	281,25	165,46	30,21	81,74	1,49	39,61	39,63	31,01	-28,18
PG2163_18-23	He	18	23	5	20,5	n	56,25	281,25	357,7	118,75	66,80	1,06	16,44	13,80	15,12	-26,95
PG2163_28-33	He	28	33	5	30,5	n	56,25	281,25	478,7	318,09	33,55	0,26	3,06	2,73	12,12	-26,35
PG2163_40-45	He	40	45	5	42,5	y	23,93	119,63	293,06	150,79	48,55	0,59	8,68	7,55	14,85	-27,13
PG2163_55-60	He	55	60	5	57,5	y	23,93	119,63	329,72	208,6	36,73	0,30	3,91	3,31	12,86	-26,49
PG2163_65-70	He	65	70	5	67,5	y	23,93	119,63	265,43	112,41	57,65	0,44	6,30	5,08	13,41	-26,21
PG2163_80-85	He	80	85	5	82,5	y	23,93	119,63	201,11	36,41	81,89	0,32	4,17	3,43	12,61	-26,12
PG2163_95-100	He	95	100	4	97	y	23,93	95,71	277,32	34,07	87,71	0,38	5,31	4,41	13,51	-26,28
PG2163_110-115	He	110	115	5	112,5	y	23,93	119,63	158,01	0,27	99,83	0,35	4,78	4,21	13,87	-26,57
PG2163_135-140	He	135	140	5	137,5	y	23,93	119,63	206,04	6,59	96,80	0,35	4,68	*	**	**
PG2163_160-165	He	160	165	5	162,5	y	23,93	119,63	206,21	8,45	95,90	0,39	5,40	*	**	**
PG2163_185-190	He	185	190	5	187,5	y	23,93	119,63	159,08	2,9	98,18	0,47	6,63	*	**	**
PG2163_210-215	He	210	215	5	212,5	y	23,93	119,63	241,75	34,97	85,53	0,38	4,97	*	**	**
PG2163_220-225	He	220	225	5	222,5	y	23,93	119,63	257,79	103,25	59,95	0,38	4,94	*	**	**
PG2155_3-8	Ko	3	8	5	5,5	n	56,25	281,25	105,39	41,21	60,90	1,08	23,01	23,01	24,92	-28,29
PG2155_11-16	Ko	11	16	5	13,5	n	56,25	281,25	220,56	165	25,19	0,28	3,60	3,12	12,98	-26,20
PG2155_20-25	Ko	20	25	5	22,5	n	56,25	281,25	523,76	395,27	24,53	0,33	4,24	3,31	11,82	-26,39
PG2155_36-41	Ko	36	41	5	38,5	y	23,93	119,63	411,29	291,19	29,20	0,40	5,38	4,63	13,61	-26,71
PG2155_45-50	Ko	45	50	5	47,5	y	23,93	119,63	264,46	141,7	46,42	0,71	11,02	9,86	16,15	-26,71
PG2155_55-60	Ko	55	60	5	57,5	y	23,93	119,63	191	55,48	70,95	0,14	1,94	1,03	8,54	-26,03
PG2155_70-75	Ko	70	75	5	72,5	y	23,93	119,63	250,15	132,83	46,90	0,13	2,04	0,80	7,35	-26,35
PG2155_83-88	Ko	83	88	5	85,5	y	23,93	119,63	255,9	116,47	54,49	0,12	1,96	0,76	7,36	-26,34
PG2155_100-105	Ko	100	105	5	102,5	y	23,93	119,63	278,57	164,53	40,94	0,13	2,03	0,85	7,75	-26,25
PG2155_130-135	Ko	130	135	5	132,5	y	23,93	119,63	284,94	121,3	57,43	0,12	2,33	0,82	8,16	-26,48
PG2155_153-158	Ko	153	158	5	155,5	y	23,93	119,63	206,59	66,96	67,59	0,12	2,38	0,78	7,35	-26,24
PG2155_165-170	Ko	165	170	5	167,5	y	23,93	119,63	200,36	52,52	73,79	0,13	2,42	0,88	8,17	-26,51
PG2155_192-197	Ko	192	197	5	194,5	y	23,93	119,63	244,44	70,44	71,18	0,16	2,29	1,13	8,35	-26,03
PG2156_1-6	Or	1	6	5	3,5	n	56,25	281,25	333,39	143,91	56,83	0,49	7,97	7,25	17,39	-28,48
PG2156_17-22	Or	17	22	5	19,5	n	56,25	281,25	633,73	77,96	87,70	0,26	3,20	2,82	12,5	-27,39
PG2156_25-30	Or	25	30	5	27,5	n	56,25	281,25	571,93	326,84	42,85	0,34	5,13	4,21	14,42	-27,72
PG2156_50-55	Or	50	55	5	52,5	y	23,93	119,63	388,64	271,56	30,13	0,17	2,15	1,31	8,97	-26,63
PG2156_65-70	Or	65	70	5	67,5	y	23,93	119,63	240,01	108,84	54,65	0,22	2,77	2,20	11,43	-27,49
PG2156_80-85	Or	80	85	5	82,5	y	23,93	119,63	214,05	101,29	52,68	0,20	3,47	2,27	13,2	-26,89
PG2156_95-100	Or	95	100	5	97,5	y	23,93	119,63	274,79	127,4	53,64	0,25	4,30	3,12	14,78	-26,91
PG2156_120-125	Or	120	125	5	122,5	y	23,93	119,63	300,14	158,24	47,28	0,22	2,96	2,31	12,2	-26,00
PG2156_140-145	Or	140	145	5	142,5	y	23,93	119,63	281,39	123,34	56,17	0,57	7,22	5,53	11,24	-26,87
PG2156_165-170	Or	165	170	5	167,5	y	23,93	119,63	304,26	152,62	49,84	0,19	2,86	1,53	9,5	-26,28
PG2156_176-181	Or	176	181	5	178,5	y	23,93	119,63	308,29	155,17	49,67	0,23	3,69	2,16	10,84	-26,48
PG2156_190-195	Or	190	195	5	192,5	y	23,93	119,63	272,27	114,45	57,96	0,21	3,59	2,10	11,44	-26,40
PG2156_215-220	Or	215	220	5	217,5	y	23,93	119,63	346,78	183,42	47,11	0,19	3,16	1,59	9,56	-26,51
PG2159_1-6	Or	1	6	5	3,5	n	56,25	281,25	313,87	89,22	71,57	1,35	25,05	25,05	21,59	-28,98
PG2159_16-21	Or	16	21	5	18,5	n	56,25	281,25	328,6	116,2	64,64	1,07	15,44	14,05	15,34	-27,82
PG2159_30-35	Or	30	35	5	32,5	y	23,93	119,63	282,11	142,84	49,37	0,76	10,75	9,83	15,11	-27,41
PG2159_45-50	Or	45	50	5	47,5	y	23,93	119,63	257,35	87,55	65,98	0,76	10,58	9,82	15,01	-27,46
PG2159_60-65	Or	60	65	5	62,5	y	23,93	119,63	323,24	153,91	52,38	0,21	3,61	2,46	13,94	-26,61
PG2159_75-80	Or	75	80	5	77,5	y	23,93	119,63	274,59	125,63	54,25	0,18	3,59	2,04	13,6	-26,23
PG2159_90-95	Or	90	95	5	92,5	y	23,93	119,63	261,74	136,23	47,95	0,22	4,08	2,65	14,18	-26,60

PG2159_105-110	Or	105	110	5	107,5	y	23,93	119,63	303,55	134,35	55,74	0,19	3,75	2,20	13,85	-26,32
PG2159_130-135	Or	130	135	5	132,5	y	23,93	119,63	220,82	59,77	72,93	0,15	3,17	1,54	11,57	-26,01
PG2159_155-160	Or	155	160	5	157,5	y	23,93	119,63	263,08	93,8	64,34	0,16	3,05	1,29	9,69	-25,75
PG2159_171-176	Or	171	176	5	173,5	y	23,93	119,63	254,93	149,58	41,32	0,12	2,84	0,78	7,56	-26,00
PG2159_195-200	Or	195	200	5	197,5	y	23,93	119,63	268,79	145,89	45,72	0,21	3,65	2,01	11,06	-25,97
PG2157_1-6	Pl	1	6	5	3,5	n	56,25	281,25	101,59	28,3	72,14	0,47	7,06	5,47	13,62	-26,84
PG2157_15-20	Pl	15	20	5	17,5	n	56,25	281,25	292,34	148,64	49,16	0,17	2,41	0,92	6,3	-26,09
PG2157_30-35	Pl	30	35	5	32,5	n	56,25	281,25	244,77	136,88	44,08	0,15	2,10	0,69	5,53	-25,57
PG2157_41-46	Pl	41	46	5	43,5	n	56,25	281,25	195,39	61,9	68,32	0,16	2,09	0,69	5,05	-25,70
PG2157_55-60	Pl	55	60	5	57,5	y	23,93	119,63	392,48	319,22	18,67	0,16	2,04	0,64	4,6	-25,67
PG2157_70-75	Pl	70	75	5	72,5	y	23,93	119,63	415,71	323,64	22,15	0,16	2,15	0,82	6,06	-25,85
PG2157_80-85	Pl	80	85	5	82,5	y	23,93	119,63	387,55	266,07	31,35	0,20	2,67	1,15	6,7	-25,88
PG2157_95-100	Pl	95	100	5	97,5	y	31,78	158,9	307,86	220,9	28,25	0,19	2,62	1,10	6,66	-25,77
PG2157_115-120	Pl	115	120	5	117,5	y	23,93	119,63	393,88	278,31	29,34	0,16	2,28	0,93	6,62	-25,71
PG2157_145-150	Pl	145	150	5	147,5	y	25,49	127,43	267,55	161,44	39,66	0,15	1,98	0,63	5,05	-25,67
PG2157_171-176	Pl	171	176	5	173,5	y	23,93	119,63	309,39	197,59	36,14	0,15	2,28	0,87	6,97	-25,92
PG2157_185-190	Pl	185	190	5	187,5	y	23,93	119,63	349,38	190,51	45,47	0,14	2,37	0,89	7,2	-25,89
PG2162_2-7	Ja	2	7	5	4,5	n	56,25	281,25	318,06	165,72	47,90	0,89	12,74	11,83	15,54	-26,7
PG2162_15-20	Ja	15	20	5	17,5	n	56,25	281,25	311,13	249,14	19,92	0,22	2,57	1,70	8,96	-25,58
PG2162_30-35	Ja	30	35	5	32,5	n	56,25	281,25	488,82	397,5	18,68	0,19	2,59	1,37	8,22	-25,56
PG2162_45-50	Ja	45	50	5	47,5	n	56,25	281,25	542,33	448,21	17,35	0,17	2,32	1,14	7,68	-25,47
PG2162_55-60	Ja	55	60	5	57,5	n	56,25	281,25	402,77	374,43	7,04	0,11	1,65	0,70	7,49	-25,96
PG2162_65-70	Ja	65	70	5	67,5	n	56,25	281,25	346,28	299,23	13,59	*	2,00	0,26	**	-25,59
PG2158_1-6	Th	1	6	5	3,5	n	56,25	281,25	475,58	413,72	13,01	0,15	1,81	0,84	6,53	-25,79
PG2158_16-21	Th	16	21	5	18,5	n	56,25	281,25	464,56	370,94	20,15	0,14	1,55	0,69	5,75	-25,65
PG2158_31-36	Th	31	36	5	33,5	n	56,25	281,25	434,72	337,96	22,26	0,14	1,57	0,68	5,63	-25,58
PG2158_46-51	Th	46	51	5	48,5	y	23,93	119,63	714,07	542,76	23,99	0,15	1,63	0,80	5,99	-25,77
PG2158_75-80	Th	75	80	5	77,5	y	23,93	119,63	406,55	295,01	27,44	0,15	1,95	1,02	7,81	-25,76
PG2158_90-95	Th	90	95	5	92,5	y	23,93	119,63	397,39	285,09	28,26	0,16	1,72	0,94	6,94	-25,80
PG2158_105-110	Th	105	110	5	107,5	y	23,93	119,63	415,43	299,99	27,79	0,16	1,60	0,94	6,94	-25,40
PG2158_125-130	Th	125	130	5	127,5	y	23,93	119,63	420,3	301,66	28,23	0,15	1,58	0,93	7,18	-25,53

**Appendix 3a:** List of explainable variable scores according the PC1 and PC2

Variables	PC1	PC2
Moisture Content	1.51	1.41
Nitrogen	2.02	-0.05
TN	2.10	-0.23
TOC	1.64	-1.16
$\delta^{13}\text{C}$	-1.90	-0.20

**Appendix 3b:** List of sample scores according the PC1 and PC2. Note that sample rows with missing values (e.g. no value due to below device-specific detection limit) were removed. 112 sample scores were calculated

Sample	PC1	PC2	Sample	PC1	PC2
J01_0-4,5	0.323937110	-0.736526780	PG2155_45-50	0.101108753	-0.148572256
PG2150_0-5	1.148170747	-1.445894686	PG2155_55-60	-0.304640798	0.483480305
PG2150_15-20	0.371682545	-0.095634243	PG2155_70-75	-0.372350617	0.129246203
PG2150_30-35	0.483811376	-0.101468684	PG2155_83-88	-0.351199015	0.268335906
PG2150_45-50	0.589955191	0.116829092	PG2155_100-105	-0.407972824	0.015548380
PG2150_60-65	0.654730332	0.242358055	PG2155_130-135	-0.325718375	0.332962501
PG2150_75-80	0.471508423	0.302575649	PG2155_153-158	-0.318439746	0.483422380
PG2150_90-95	0.524615032	0.412157204	PG2155_165-170	-0.260695134	0.588425964
PG2150_115-120	0.488935186	0.494218415	PG2155_192-197	-0.297738035	0.511503916
PG2150_140-145	0.201193098	0.420410344	PG2156_1-6	0.391677256	-0.296283571
PG2150_165-170	0.179771087	0.279637223	PG2156_17-22	0.054447730	0.650588622
PG2150_190-195	0.102135596	0.416362715	PG2156_25-30	0.004133377	-0.060479548
PG2150_215-220	0.036118583	0.196718170	PG2156_50-55	-0.359608926	-0.233477135
PG2151_0-5	1.233745183	-1.179939403	PG2156_65-70	-0.098936329	0.268308268
PG2151_15-20	0.742279355	-0.137415990	PG2156_80-85	-0.188460021	0.204612895
PG2151_31-36	0.743586221	-0.070379597	PG2156_95-100	-0.139702865	0.202146362
PG2151_45-50	0.745507377	0.161444095	PG2156_120-125	-0.309845211	0.065724053
PG2151_61-66	0.891183768	0.272481090	PG2156_140-145	0.022809931	0.194536920
PG2151_76-81	0.596254449	0.310450925	PG2156_165-170	-0.311255299	0.162873920
PG2151_90-95	0.495196700	0.502377491	PG2156_176-181	-0.246365960	0.152704249
PG2151_105-110	0.397701779	0.597565032	PG2156_190-195	-0.236061885	0.293931660
PG2151_130-135	0.374840228	0.530581681	PG2156_215-220	-0.289303146	0.131786198
PG2151_155-160	0.574194810	0.436615644	PG2157_1-6	0.182663618	-0.054408777
PG2151_180-185	0.211565673	0.484258985	PG2157_15-20	-0.348375569	0.088718018
PG2151_205-210	0.250186125	0.575556281	PG2157_30-35	-0.464517074	0.010625218
PG2151_230-235	0.098141902	0.255605188	PG2157_41-46	-0.357104077	0.434879769
PG2152_9-14	-0.141715710	-0.444398182	PG2157_55-60	-0.576171250	-0.545174137
PG2152_21-26	-0.334923776	-0.546035324	PG2157_70-75	-0.527429261	-0.442010869
PG2152_29-34	-0.383481584	-0.511334567	PG2157_80-85	-0.441071121	-0.231864602
PG2152_40-45	-0.198025610	-0.385297213	PG2157_95-100	-0.476079043	-0.302198443
PG2152_54-59	0.090817607	0.136828991	PG2157_115-120	-0.501702786	-0.266863204
PG2154_2-7	1.315650032	-0.742596992	PG2157_145-150	-0.486277009	-0.029048637
PG2154_13-18	0.567152568	-0.052308675	PG2157_171-176	-0.459968727	-0.094214593
PG2154_25-30	-0.048498875	-0.334835066	PG2157_185-190	-0.422959941	0.088204908
PG2154_40-45	0.187226932	0.140153744	PG2158_1-6	-0.547593604	-0.903077918
PG2154_53-58	0.295403501	0.259349924	PG2158_16-21	-0.567772940	-0.544854031
PG2154_81-86	0.176552368	0.826511385	PG2158_31-36	-0.570790763	-0.467335731
PG2154_100-105	0.091361617	0.837038985	PG2158_46-51	-0.527782420	-0.408392028
PG2154_175-180	0.106017428	0.866286066	PG2158_75-80	-0.504278285	-0.321968735
PG2154_192-197	0.094330779	0.869768955	PG2158_90-95	-0.496408180	-0.292364114
PG2155_3-8	0.775175994	-0.641421564	PG2158_105-110	-0.548043511	-0.324716386
PG2155_11-16	-0.294475672	-0.564940953	PG2158_125-130	-0.536284745	-0.301796710
PG2155_20-25	-0.266237656	-0.527774612	PG2159_1-6	1.049929365	-0.748244936
PG2155_36-41	-0.158318864	-0.395440169	PG2159_16-21	0.485903442	-0.006687873



Sample	PC1	PC2
PG2159_30-35	0.221916405	-0.097380392
PG2159_45-50	0.274149460	0.225468849
PG2159_60-65	-0.211597509	0.163518199
PG2159_75-80	-0.281882367	0.196905271
PG2159_90-95	-0.223347774	0.095151954
PG2159_105-110	-0.258918628	0.233790180
PG2159_130-135	-0.278559389	0.513247634
PG2159_155-160	-0.347544134	0.380463894
PG2159_171-176	-0.446296636	0.021532155
PG2159_195-200	-0.336874441	0.057453596
PG2162_2-7	0.327476393	-0.695889647
PG2162_15-20	-0.484010675	-0.638420421
PG2162_30-35	-0.530268010	-0.616522655
PG2162_45-50	-0.574970561	-0.631846668
PG2162_55-60	-0.658719383	-0.944674423
PG2163_3-8	1.110635290	-0.718060655
PG2163_18-23	0.376698862	-0.001728040
PG2163_28-33	-0.276379981	-0.269335329
PG2163_40-45	0.092883387	-0.046596866
PG2163_55-60	-0.224268675	-0.174558183
PG2163_65-70	-0.087068544	0.150446111
PG2163_80-85	-0.104725893	0.566035680
PG2163_95-100	-0.024461422	0.637399913
PG2163_110-115	0.027406291	0.824568834

## 9. Danksagung

Mein größter Dank, viel Respekt und Anerkennung gehen an meinen Betreuer am Alfred-Wegener-Institut in Potsdam, Dr. Michael Fritz. Während meiner Schreibzeit am Institut war er ein stetiger Ansprechpartner, hatte auf alle meine relevanten und irrelevanten Fragen eine perfekte Antwort und brachte täglich gute Laune in das Büro. Sein fundiertes Wissen zu Herschel Island, aber auch zu interdisziplinären Themen und seine stetige Kommunikationsbereitschaft steigerten meine Begeisterung für die Polargebiete und brachten mich in meiner Arbeit stetig voran.

Ein Dankeschön für das Vertrauen geht auch an Prof. Dr. Hughes Lantuit, der als Leiter der Arbeitsgruppe COPER und damit Entscheidungsträger in der Vergabe des Themas mir das Schreiben dieser Arbeit ermöglichte.

Meinem Entschluss, ein Thema am AWI zu wählen, ging neben meinem starken Interesse an der Forschungsarbeit und der persönlichen Verbundenheit zur kanadischen Natur auch ein Praktikum an diesem Institut voraus. Während dieser Zeit wurde meine Begeisterung für die Wissenschaft durch spannende Laborarbeit und erste Einblicke in den Forschungsalltag weiter verstärkt. Besonderer Dank geht dazu an die Laborleiterin Frau Ute Kuschel, die mir während dieser Zeit eine stetige Ansprechpartnerin war und damit meinen Entschluss zu dieser Arbeit mit initiierte. Weiterhin danke ich Jaroslav Obu aus der COPER Arbeitsgruppe für die kontinuierliche Unterstützung und Bereitstellung seiner fundierten Feld- und Laboraufzeichnungen zu Herschel Island. Auch an das restliche COPER-Team geht ein herzlicher Dank für eine lustige Zeit am Institut mit viel Kaffee.

Vielen Dank an Romy Zibulski und Bastian Niemeyer für die Einführung in die Welt der multivariaten Statistik.

Das hohe Maß an zeitlicher und finanzieller Freiheit, das mir während dieser Zeit zur Verfügung stand, wäre kaum möglich gewesen ohne die Unterstützung meiner lieben Familie. Vielen Dank an meine Eltern und an meine Schwester, die mir ermöglicht haben, für ein Großteil der Zeit direkt am AWI arbeiten zu können. Ich liebe euch!

Zu guter Letzt danke ich Prof. Dr. Matthias Hinderer für die Unterstützung dieser Kooperationsarbeit und seinen vorausgegangen Kartierkursen, welche die Geologie für mich zu mehr als einer Wissenschaft machten.

## **Eidesstattliche Erklärung**

Hiermit erkläre ich, Stefan Baltruschat (Matrikel-Nr. 1712083), dass ich die vorliegende Bachelorarbeit

"Soil organic matter and stable carbon isotopes in surficial permafrost on Herschel Island, Yukon Territories, Canada"

ohne Hilfe Dritter und ohne Benutzung anderer als der angegebenen Hilfsmittel angefertigt habe; die aus fremden Quellen direkt oder indirekt übernommenen Gedanken sind als solche kenntlich gemacht. Die Arbeit wurde bisher in gleicher oder ähnlicher Form keiner anderen Prüfungsbehörde vorgelegt und nicht veröffentlicht.

.....

Ort, Datum

.....

Unterschrift

Erstberichterstatter/in: Prof. Dr. Matthias Hinderer

Zweitberichterstatter/in: Dr. Michael Fritz